DESIGN AND ANALYSIS OF A COMPACT TWO PHASE COOLING SYSTEM FOR A LAPTOP COMPUTER

A Thesis

Presented to

The Academic Faculty

by

Adya Alisha Ali

In Partial Fulfillment
of the Requirements for the Degree
Master of Science in Mechanical Engineering

Georgia Institute of Technology
June 2004

DESIGN AND ANALYSIS OF A COMPACT TWO PHASE COOLING SYSTEM FOR A LAPTOP COMPUTER

Approved by:

Dr. Yogendra Joshi, Advisor

Dr. Sheldon Jeter

Dr. S. Mostafa Ghiaasiaan

Date Approved: Friday July 9th, 2004

To My Family

ACKNOWLEDGMENTS

I graciously thank my advocate and advisor, Dr. Yogendra Joshi, whose wisdom, guidance and faith in me have seen me through the steps of the entire graduate school process. I thank my committee members, Dr. Sheldon Jeter and Dr. S. Mostafa Ghiaasiaan for their service, time and understanding. I am grateful to my colleagues at Georgia Tech, in particular the members of the Microelectronics and Emerging Technologies Thermal Laboratory (METTL), for their support and help with various aspects of this project. Thanks to my non-technical friends for their belief in me and for being my cheerleaders from afar. Special mention must be given to some very dear friends, Wayne Johnson, Karen Davis, and Donavon Gerty, for their continuous encouragement, support and compassion through my graduate school years. Finally I would like to express my gratitude to my family for their complete faith in me, and for giving me strength and love through this incredible experience.

This project was made possible through generous funding and support from The Institute of Microelectronics, Singapore.

TABLE OF CONTENTS

LIST OF FIGURES

LIST OF TABLES

ABSTRACT

Technological advancement, as well as consumer demands, has motivated the miniaturization of electronic/mechanical systems and increase of device power and performance. The notebook computer is not an exception, and innovative thermal management solutions must be employed to compensate for the increased heat dissipation in the space-constrained enclosures. The majority of current cooling systems in laptop computers rely on heat pipes attached to a remote heat exchanger with micro-fans providing forced convection to reject heat to the ambient, however this technique can not accommodate the increasing heat fluxes in the confined laptop enclosure.

In this study, a two-phase closed loop cooling system is designed and tested for a laptop computer. The cooling system consists of an evaporator structure containing boiling structures connected to a compact condenser with mini fans providing external forced convection. A pump is also incorporated to assist the return of the condensate back to the evaporator. The cooling system is characterized by a parametric study which determines the effects of volume fill ratio of coolant, initial system pressure, and pump flow rate on the thermal performance of the closed loop. Experimental data shows the optimum parametric values which can dissipate 25 W of chip power with a chip temperature maintained at ? 95 ?C.

Numerical analysis provides additional data to further enhance the heat dissipation from the external air-cooled side of the condenser by studying the effects of ventilation and air flow rate across the system. Thermal management of mobile systems must be considered

during the early design phases, and this research shows the feasibility of implementing of a two-phase cooling system to dissipate 25 W in a laptop computer.

CHAPTER I

INTRODUCTION

Portable computers have improved significantly since their conception and introduction into the market in the 1980s. Advances in technology as well as demands from the consumer have led to thinner, lighter and higher performance notebook computers. The central processing unit (CPU) acts as the "brain" of the laptop and is responsible for all the operations of the computer. Continuous improvement in CPU power, in addition to volume and weight constraints, has made effective thermal management concepts a necessity in notebook design. Earlier generations of microprocessors required minimum or no thermal management. New-generation microprocessors have become increasingly smaller and more powerful, and have shown a rapid increase in total power dissipation. These higher heat fluxes have created a demand for new thermal management techniques.

There are two main elements of thermal management: component level cooling and system level cooling. The former is a cooling solution in contact with the processor that must spread the heat to reduce the heat flux. System level cooling maximizes heat dissipation from the system's walls or shell to the environment. Component level cooling includes heat sinks or heat exchangers attached to the CPU chip, while system level cooling may incorporate a fan ducted to a remote heat exchanger connected to the thermal die with a heat pipe.

The miniaturization of the notebook enclosure, as well as increased heat output of internal components, has caused higher internal air temperatures and component temperatures. As a result, more effective thermal management concepts are required to enable faster clock rates and increased heat dissipation at chip levels. Thermal issues on a system-wide basis need to be addressed during the early stages of the design process to ensure efficient and cost effective cooling of notebook computers.

1.1 Thermal Management of Computers

Technical advances fueled the evolution of the mainframe (1960s), to the minicomputer (1970s) to the personal computer (PC) (1980s). The PC gained popularity and acceptance through its user-friendly application software, communication capabilities and competitive prices; however, the PC lacked the key feature of mobility. The Osborne portable computer was one of the first to be shipped but was still too heavy with a weight of 26 pounds [1]. Smaller laptops have developed through innovative technology and knowledge in miniaturization. Current mobile processors speeds are as high as 3.2 GHz, while thickness and weight of some notebook computers on the market are even less than 25.4 mm and 15 kg respectively [2].

Miniaturization of a system such as a notebook computer is achieved by fitting several functional components into a limited space where constraints such as size, weight, reliability and cost, drive the need for more complex thermal management in mobile computers. Consideration must also be given to the various types of environment in which mobile computers might be used. The geometry of component layout provides a variety of heat path configurations and different length scales to dissipate heat.

A processor is typically designed to meet a specific thermal design power (TDP). The thermal solution is required to dissipate the TDP (maximum power consumption of a processor) although the value represents the worst case real application which is very rarely attained by an average user. The ultimate goal of thermal management is to dissipate the TDP and maintain the processor below its maximum operating temperature (T_{case}). Thermal monitoring of the hottest location on the die determines the maximum junction temperature (T_j). Major laptop manufacturers have successfully employed thermal management techniques for mobile processors with an average TDP of 20 W such as the Intel Mobile Pentium III processor with a maximum TDP of 21.5 W [3]. Most recently (January 2004) Intel Corporation introduced the Intel Celeron M processor for mobile computers with a TDP of 24.5 W [4]

Cooling solutions for notebook computers are usually more complex, with limited space and varying design layouts, than for desktop systems. Although the cooling solutions may vary among manufacturers, all notebook computers employ passive and/or active cooling methods with either air or liquid coolants. A basic passive cooling method is natural convection within the laptop cabinet whereas an active cooling method employs fans to aid airflow over the devices in the laptop cabinet. A combination of fan and heatsink can sufficiently cool low-power (<8 W) mobile processors.

A passive heat sink is simply a mass of thermally conductive material in contact with the heat source where the heat is drawn away from the source and into the air stream. Heat sinks are typically designed with extended surfaces, such as pin fins, to increase the surface area. A passive heat sink is cost effective and reliable; however it

may remove only a limited amount of TDP. Adding a small fan directly to the heat sink provides airflow to the critical device.

1.2 Liquid Cooling Technology

Although air-cooling is widely used in cooling methods for electronic packages, it is known that liquid cooling can accommodate significantly higher heat fluxes due to higher specific heat and thermal conductivity. Liquid cooling methods for microelectronics can be categorized as either indirect or direct. Indirect liquid cooling prevents any contact between the microelectronic components and the coolant. In these cases it is necessary to provide a good thermal conduction path from the microelectronic heat sources to the liquid. Water is the preferred coolant for indirect liquid cooling because of its superior thermophysical properties (Table 1) whereas fluorocarbon liquids (e.g. FC-72, FC-86) are more suitable for direct cooling on account of its chemical characteristics.

Table 1 Comparison of thermophysical properties of flourocarbon coolants and water [5]

PROPERTY	FC-72	FC-77	H_20
Boiling point at 1 atm (?C)	56	97	100
Density x 10^{-3} (kg/m^3)	1.680	1.780	0.997
Specific heat x 10^{-3} (W-s/kg-K)	1.088	1.172	4.179
Thermal conductivity (W/m-K)	0.0545	0.057	0.613
Dynamic viscosity x 10^4 (kg/m-s)	4.50	4.50	8.55
Heat of vaporization x 10^{-4} (W-s/kg)	8.79	8.37	243.8
Surface tension x 10^3 (N/m)	8.5	8.0	58.9
Thermal coefficient of expansion x 10^3 (K^{-1})	1.6	1.4	0.2
Dielectric constant	1.72	1.75	78.0

Direct liquid cooling; also referred to as immersion liquid cooling, defines the cooling method in which the microelectronics are directly in contact with the coolant. Since there is no wall separating the heat source from the coolant, the heat can be removed directly from the chip, therefore eliminating the additional thermal conduction resistance caused by contact with a wall. Direct liquid immersion cooling provides a higher heat transfer coefficient, however the coefficient's magnitude depends on the specific coolant and mode of convective heat transfer. Although several coolants can provide adequate direct cooling, consideration must given to the coolant's chemically compatibility with the chip and other packaging materials exposed to the liquid.

The relative magnitude of heat fluxes accommodated by liquid cooling depends on convective heat transfer processes classified as natural convection, forced convection, or boiling modes. Natural convection heat transfer arises from the mixing and fluid motion induced by density differences of the coolant. Liquid natural convection attains low heat transfer rates, which can be exceeded by forced convection heat transfer mode in which a pump is utilized to increase the velocity of the liquid over the heated surface. Boiling is a convective heat transfer process that depends on the phase change of the working fluid where vapor bubbles form at the heated surface and is commonly referred to as either pool boiling or flow boiling.

The boiling curve (Figure 1) for a typical fluorocarbon coolant shows the magnitude of heat fluxes as a function of 'wall superheat'. At low chip powers, natural convection (A-B) begins the heat transfer process until sufficient superheat is available to initiate bubble growth on the surface, at which point boiling begins. As the power is

increased, more nucleation sites become active and bubbles depart more frequently thereby increasing the fluid circulation near the chip. The region between B and C is termed the nucleate boiling regime where increased fluid circulation caused by the motion of the vapor bubbles provide the ability to accommodate higher heat flux with minimal increase in surface temperature. Section D-E shows the transition to film boiling in which the heat transfer depends on conduction through the vapor. Heat transfer in this region is very poor and may results in electronic failure due to high temperatures. The most desirable mode for electronics cooling is the nucleate boiling regime.

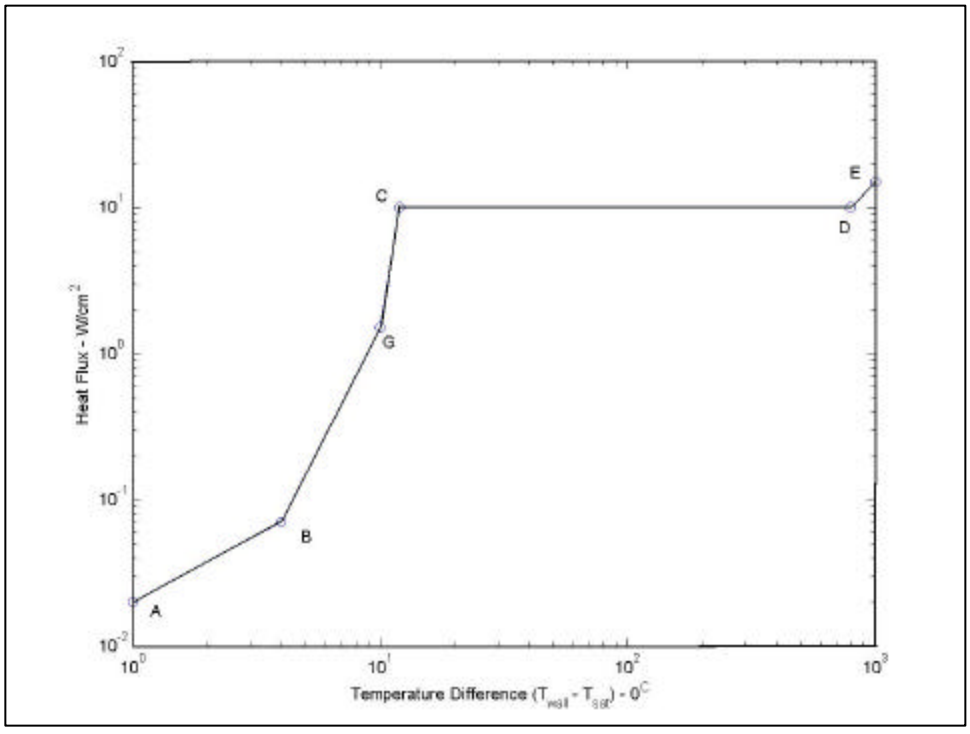

Figure 1 Typical heat transfer regimes for immersion cooling with a fluorocarbon [6]

Direct and indirect liquid cooling methods can each be further categorized into single-phase and two-phase liquid cooling. As an example, jet impingement cooling may be utilized as a two-phase direct method, in contrast to the two-phase indirect technology of heat pipes and thermosyphons. Two-phase cooling methods are more desirable because of high heat transfer coefficients, however the systems tend to be more complex. In the mid 80s, IBM employed indirect liquid cooling technology using water for mainframes and supercomputers. This technology then became the norm for high performance computers which easily accommodated the large cold plates and heat conduction devices. In large mainframe computers the cold plates (containing water) can be sufficiently separated from the electronics and thermally connected with heat conduction devices. Two-phase cooling was not considered for notebook computers at that time since most microprocessors were sufficiently cooled with metallic heat sinks and fans.

1.2.1 Two Phase Cooling Systems

Heat pipes provide a passive two-phase heat transfer method to transmit heat from confined spaces to a condenser. A heat pipe is an evacuated and sealed metallic vessel partially filled with a small amount of working fluid (typically water or methanol) which vaporizes as heat is applied to the metal surface (Figure 2). The resulting pressure gradient forces the vapor to the cooler section of the heat pipe where it condenses and releases latent heat. Wick structures on the inner walls of the heat pipe provide capillary forces to pump the condensate back to the hot end of the heat pipe completing the

continuous evaporation/condensation cycle. The types of wick structures, such as extruded grooves, screen mesh, and powdered metal, are crucial in providing the capillary pumping action to circulate the fluid. Copper tubing is the most common material used to make heat pipes due to the material's compatibility with common working fluids, high thermal conductivity, and manufacturability. Flattening the tubes allows heat pipes to interface with flat surfaces and minimize thermal contact resistance. Structure, shape and length are also factors that affect the heat pipe's performance,

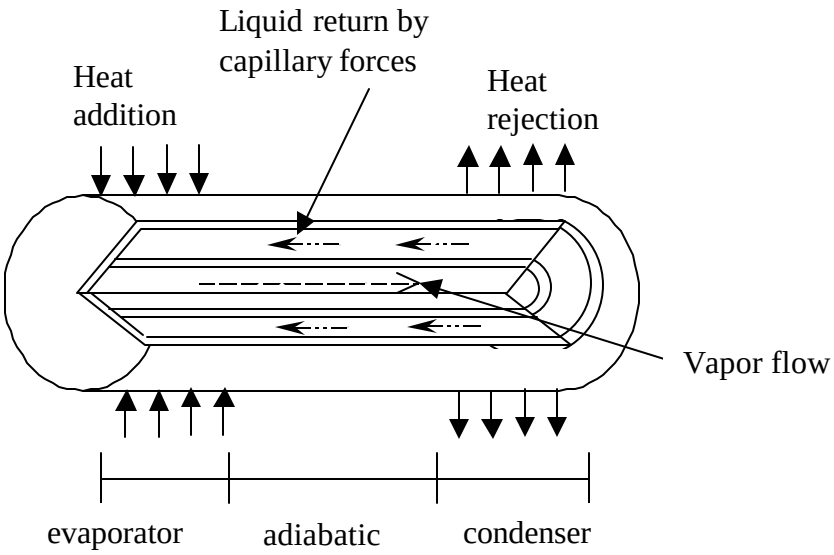

Figure 2 Structure and principle of heat pipe

The first implementation of a heat pipe in a notebook computer occurred in 1994 despite the fact that the first working heat pipe was built in 1963 [7]. Earlier notebook computers relied on simple metallic heat sinks, but by the late 1990s approximately 60% of notebook computers used heat pipes in thermal management solutions [7]. It is now common to find heat pipes in different configurations used in thermal solutions for

portable computers. Advantages of heat pipes include their simple structure, light weight, no mechanical components, and no power consumption. Heat pipes typically transfer heat away from the CPU and dissipate the heat through larger areas such as components located in the base of the laptop (keyboard and chassis). However, there is a limit to the amount of power dissipation achievable through a sole heat pipe in the base. Xie et al estimated a maximum of 6.54 W (4 W from board, 0.5 W each for HDD and power supply) of power could be dissipated through the base [8].

Mochizuki et al (1997) [9] designed and tested a hinged heat pipe cooling system that utilizes the back of the liquid crystal display screen (LCD) of a notebook computer. A primary heat pipe (4 mm OD) in contact with the CPU transfers heat through a hinge to a secondary heat pipe (3 mm OD). This second heat pipe transfers the heat onto an aluminum heat spreader plate (250 x 174 x 0.4 mm), which dissipates it into the back of the LCD. The hinged copper connector enables heat transfer between the two copper heat pipes and allows easy opening and closing of the notebook cover. The dimensions for both heat pipes were based on thermal resistance predictions to maintain a case temperature of = 95 ?C with an ambient temperature of 40 ?C behind the LCD. Experiments showed the capability of the hinged heat pipes in the 10 – 12 W range of input heat. A hinged heat pipe system used as an auxiliary cooling solution to an existing heat dissipation solution under keyboard can cool a minimum of 12 W. Since the late 1990s a similar hinged heat pipe system has been incorporated in the commercially available IBM Thinkpad mobile computers (Figure 3).

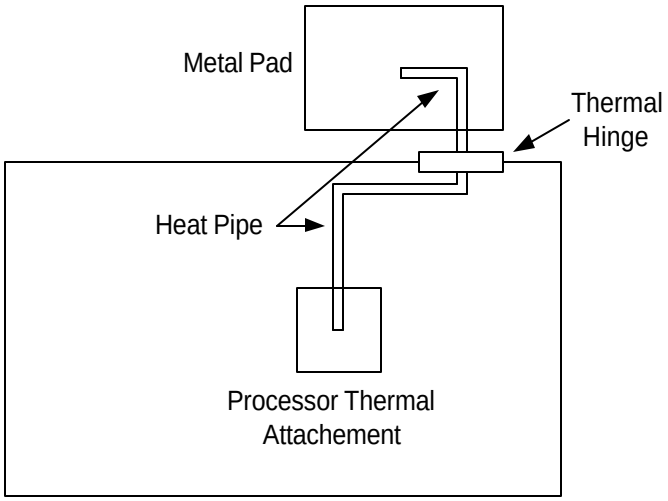

Figure 3 Schematic of Thermal Hinge System in IBM Thinkpad T series [10]

Another common mobile thermal solution is a remote heat exchanger system: a combination of heat pipe, heat sink, and fan. Nguyen et al (2000) tested the concept with a copper heat block, copper heat pipe, and aluminum heat sink. One end of the 6mm round flattened heat pipe is attached to the heat block (30 x 30 x 3 mm), and the other end is attached to the base of the aluminum heat sink (? 100 cm^2 total fin surface area). A fan (50 x 50 x 9 mm) provides forced airflow through the heat sink as shown in Figure 4. The remote heat exchanger system can dissipate 20 W with a junction temperature limit of 90 ?C and ambient of 40 ?C [11].

In the mid 1990s Intel used the heat pipe with spreader alone (Figure 5), but later replaced it with the remote heat exchanger system implemented in Intel Mobile Pentium III cooling technology with an average TDP of 20 W [12]. The Toshiba Portege 3480CT notebook computer uses a different configuration of the remote heat exchanger where a magnesium heat sink draws heat away from the chip surface. Water vaporization occurs

in the hot end of the copper tube (attached to heat sink), and heat is spread through the aluminum plate as the vapor cools (Figure 6).

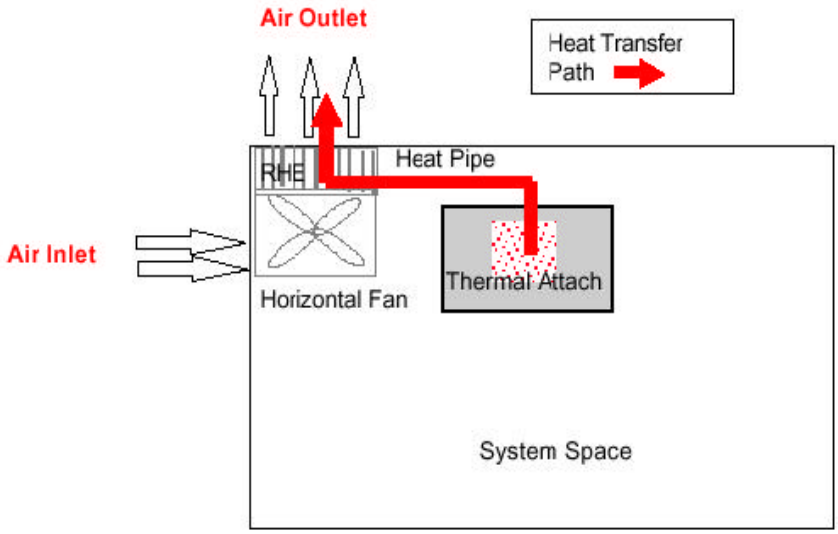

Figure 4 Schematic of a typical remote heat exchanger system [12]

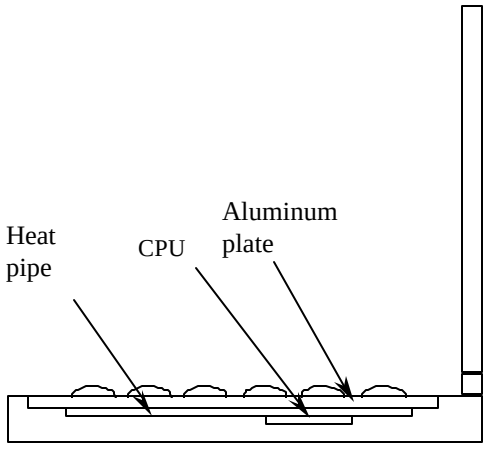

Figure 5 Heat pipe and heat spreader plate under keyboard [13]

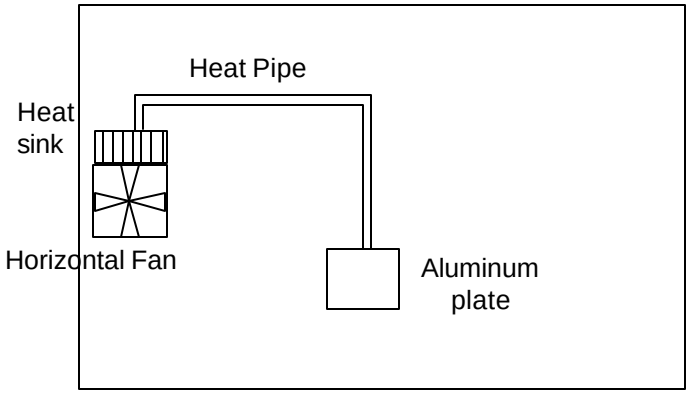

Figure 6 Schematic of cooling system for Toshiba Portege

Chip powers in excess of a few tens of W are beyond the capacity of conventional heat pipes even with remote heat exchangers. The limiting factors in the heat pipes are the wick thickness (capillary forces) and the cross-sectional area. In 1994 Aavid Engineering demonstrated its two-phase passive cooling system, known as Oasis technology, for notebook computers [14]. Fluid contained in a sealed unit is heated by the chip and vaporizes. Natural convection effects force the vapor to travel to a thin chamber behind the display screen where it condenses and flows back down to the high temperature chip. The passive system reportedly accommodated a heat flux of 29 W/cm^2 with an estimated junction temperature of 110 ?C, however other specifications, such as size and weight, were not published.

In an effort to provide an alternative to heat pipes, Jiang et al. [15] developed and tested a closed-loop two-phase microchannel cooling system using electroosmotic pumping for the working fluid (1 mM buffered deionized water). The cooling scheme for VLSI chip application consists of a microchannel heat exchanger above the chip, a heat rejector placed downstream of the heat exchanger and an electroosmotic pump which

returns cooled liquid back into the heat exchanger (20 mm x 29 mm x 500 ?m). A pressure transducer provides the pressure drop across the microchannel heat exchanger while the heat rejector consists of an aluminum heat sink with embedded flow channels and a fan. The pump was characterized by a linear relationship between flow rate and back pressure, where it delivered a maximum flow rate of 7 ml/min and maximum pressure of 160 kPa. The two-phase system accommodated up to 38 W/cm^2 of input power giving a junction-fluid thermal resistance value of about 0.1 K/W. The chip temperature was maintained below 120 ?C, with a pressure drop of 30 kPa at 38 W and an estimated saturation temperature of 110 ?C.

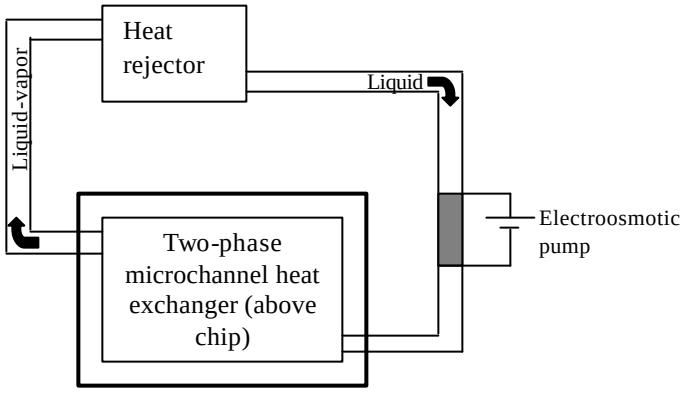

Figure 7 Schematic of electroosmotic cooler [15]

The new Hitachi Flora 270W silent model is a liquid-cooled notebook computer, which also utilizes the backside of the display screen and a micropump [16]. A liquid cooling jacket removes heat from the chip and the liquid is then pumped to the backside of the display screen where heat is dissipated from a radiator panel. The radiator panel is connected with flexible tubes to a reserve tank that supplies cooled liquid back to the

chip. A prototype pump made of hard resinous material with glass fiber provided a flow rate of 650 ?l/sec and static pressure of 6 kPa at 35 ?C by a rubbing action. The radiator panel dissipated 30 W of heat, while an additional 10 W and 20 W were dissipated through the keyboard and laptop chassis respectively. The fanless system eliminated the acoustic noise associated with fans found in conventional forced air-cooled systems. In 2002 Hitachi Ltd commercialized the first long-life, water-cooling system for a high performance Mobile Intel Pentium Processor-M.

1.3 Summary and Overview of Current Study

Thermal management solutions for portable computers have evolved from simple heat sinks with forced air-convection to micro heat pipes and remote heat exchangers to accommodate higher heat fluxes in newly designed mobile computers. In the last decade, several configurations of heat pipes and remote heat exchangers adequately maintained a ? 100 ?C junction temperature while dissipating an average of 20 W from the mobile processors. However, for even higher heat dissipation novel thermal management ideas must be developed.

Recently, two-phase flow loops employing boiling in small channels or tubes have been attempted, but the concept of boiling with enhancement structures has not been tested for compact evaporator cavities suitable for a laptop computer. The design of the condenser section is also addressed in developing a two-phase closed loop cooling system with constraints on size, weight and power consumption.

Chapter 2 describes the design of the main components for the two-phase system and the fabrication methods used. The experimental procedure details are given along with calibration data for the thermal test board and thermocouples.

Chapter 3 provides a numerical analysis of the condenser design where the design is evaluated in terms of velocity and temperature distribution, as well as the total heat transfer rate.

Chapter 4 examines the experimental results from a two-phase cooling system. A parametric study is conducted to study the effects of most operating parameters, including fill ratio, internal pressure and liquid flow rate, on the thermal performance of the system.

CHAPTER II

FABRICATION AND EXPERIMENTAL PROCEDURE

This chapter introduces the design details of the closed loop cooling system including the fabrication methods for the main components: evaporator with enhanced boiling surfaces and condenser. The thermal performance of the cooling system was determined by measuring the power dissipated from the chip while maintaining a junction temperature (T_j) of ? 95?C) and was evaluated by testing the effect of design parameters such as the volume of liquid in the system, initial system pressure, and internal liquid flow rate. The closed loop system (Figure 8) starts at the evaporator attached to the thermal test chip, and joins to a remote serpentine finned-tube condenser located near some enclosure vents with two mini vertical fans providing external forced convection across the condenser.

The evaporator contains layers of three-dimensional copper structures, which reduce the incipience overshoot and increase the critical heat flux. Nakayama et al. (1984) [17], used similar enhanced surface structures in a pool boiling study and these structures were also used more recently for the two phase closed loop cooling of a desktop system where a total of 85 W could be accommodated by larger evaporator and condenser components (scale factor of 2) [18]. The compact evaporator and condenser in this study were designed based on size constraints and computational modeling of the air flow across the condenser. Initial experiment data showed poor results with a gravity-driven loop therefore a modification was made in the design and the parametric study was

conducted as a pump-driven closed loop cooling system. The following sections describe the design and fabrication of each component, and provide details about the experimental procedure, data acquisition, and uncertainty analysis.

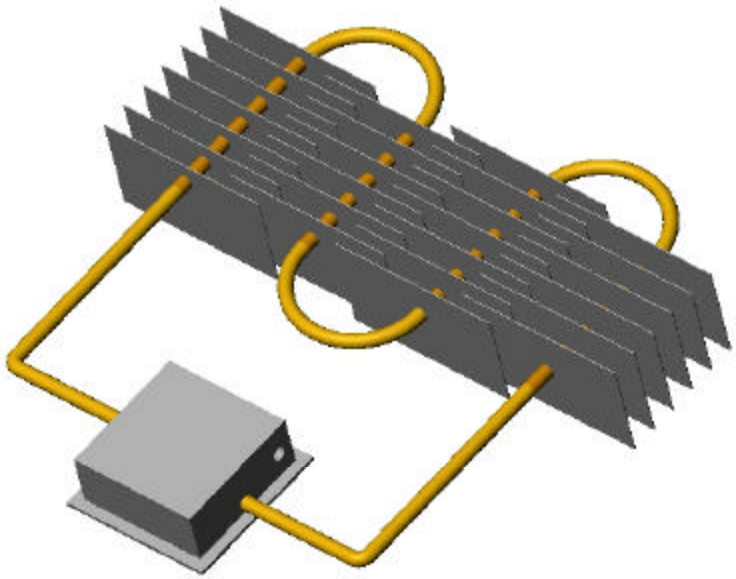

Figure 8 Isometric view of the two-phase closed loop cooling system

2.1 Fabrication

2.1.1 Enhanced Copper Structures

The evaporator is a major component of the thermosyphon loop in which the heat from the source vaporizes the working fluid. Boiling enhancement copper structures [17] are used in the evaporator to increase the surface area of the heat source. The structures are based on the theory of nucleate boiling in which the temperature difference between the evaporator wall and working fluid govern the formation of bubbles. The structures are fabricated from a 0.8 mm thick sheet of copper by wire electrical discharge machining (EDM); a process that uses an electrically charged wire brought close in

proximity to the oppositely charged copper sheet. The resulting electrical discharge removes pieces of the copper forming channels with a width (W_t) of 0.31 mm and a depth (H_t) of 0.55 mm. The channels are machined on both sides in perpendicular directions to form nucleation sites (pores) on the copper strip. An accurate fabrication process would create perfectly rectangular channels which ultimately maximize the area of the nucleation sites and improve the efficiency of the structures, however, the enhancement structures used in this study

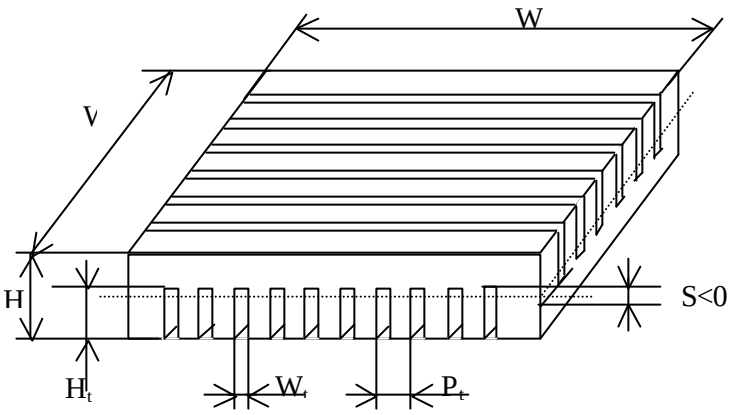

Figure 9 Schematic of Boiling Enhancement Structure

Figure 10 Picture of a single copper structure used in the experiments

The boiling enhancement structures are most effective when placed above the heat source, therefore the strip is cut into several pieces measuring 12 x 12 mm, which is equivalent to the surface area of the thermal test chip. Individual structures are oxidized on a hot plate at 200 ?C after which the top and bottom surfaces are polished leaving the channels still oxidized. Three structures are stacked with layers of solder between them but the pores remain visibly clear due to the oxidation process. The solder is reflowed at 221?C (Pb-Sn liquidus temperature) to form a three-dimensional boiling enhancement structure, with a total height of 2.6 mm. The stack of structures is then soldered to the base plate of the evaporator cavity.

2.1.2 Evaporator Section

The evaporator cavity, which contains the boiling enhancement structures submerged in working fluid, should provide good thermal contact with the thermal test chip and enhance heat transfer to the fluid. Copper has thermal conductivity and density values of 8933 kg/m^3 and 401 W/m-K respectively, compared to Aluminum with a density of 2770 kg/m^3 and thermal conductivity of 190 W/m-K. The advantage of copper is in its 45% increase in conductivity over aluminum, however the counter effect is its 70% increase in density. Considering the volume of the entire compact system, the conductivity is more essential and therefore the evaporator and condenser are fabricated from the higher conductive copper. The copper is nickel-plated simply to prevent oxidation of the copper, and provide a smoother mating surface as a side benefit.

The base plate has dimensions of 35 x 35 x 1 mm thick with the copper structures attached in the middle. The evaporator case (30 x 30 x 8 mm) is a five-sided cube with a 0.5 mm thick top wall, and sidewalls of 2 mm thickness. Two 3.2 mm hollow copper tubes provide a connection from the evaporator to the inlet and outlet of the condenser. One tube is slightly elevated to aid the escape of vapor bubbles, while the lower tube enhances liquid flow back to the evaporator. The copper case is then soldered to the base plate to form the evaporator cavity. The height constraint in a laptop cannot accommodate a large evaporator; therefore the evaporator was designed to maximize the internal volume in a confined space.

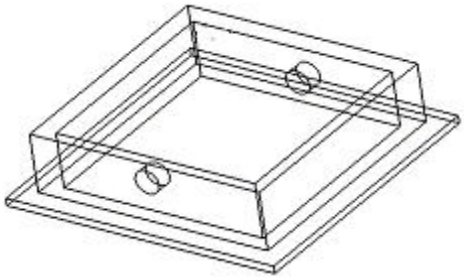

Figure 11 Isometric wireframe view of evaporator case without boiling structures

2.1.3 Condenser Section

Heat exchangers have been a key component in the heat transfer process of common devices such as refrigerators, car radiators and even power plants. There are several configurations of heat exchangers which are basically used to transfer heat between two fluids. Specifically, compact heat exchangers are devices with a dense array of extended surfaces packed into a small volume of space, and are typically used when at least one of the fluids is a gas. In this case the vapor entering the condenser must transfer

heat to the surrounding air and condense into liquid state which returns to the evaporator. Fans provide external forced flow over the fins to further enhance the heat transfer. Nickel-plated copper is also used to fabricate the serpentine fin-tube condenser to allow easier connection to the evaporator.

Fin-tube bonding techniques may vary across manufacturers; however it is always essential to minimize the thermal resistance between the fins and tubes. Each plate was first punctured with a hole slightly smaller than the tube's external diameter (3.2 mm). The plates were positioned on the tubes (6 mm fin spacing) and soldered at the plate-tube joints onto two U-shaped tubes, which were later connected with a smaller U-shaped tube to form the serpentine condenser. The benefit of the offset fin design is an induced turbulence and higher heat transfer coefficient, however the pressure drop across the condenser also increases and may not be compensated by small fans. Figure 12 and Figure 13 show the isometric and top views of the condenser respectively. There is a slight gradient in the condenser tubes to assist flow from the inlet to the outlet.

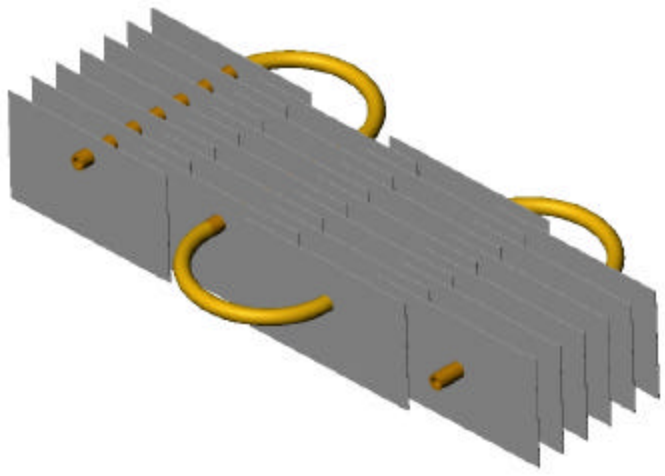

Figure 12 Compact serpentine fin-tube condenser

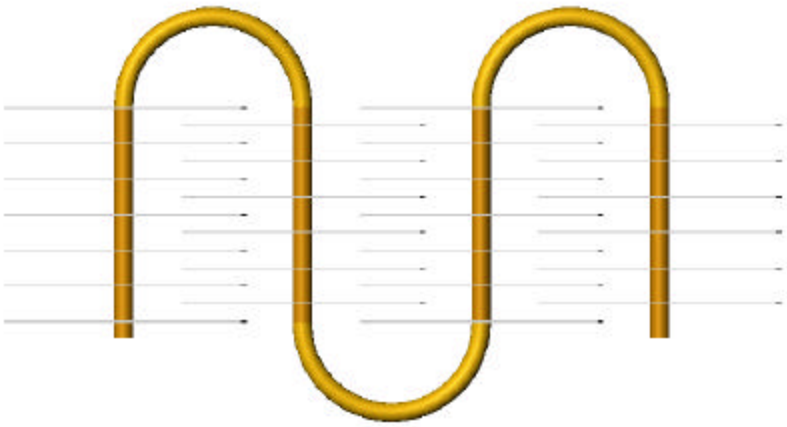

Figure 13 Top view of serpentine condenser

2.2 Calibration Methods

In experimental work it is necessary and important to calibrate equipment and other apparatus to assess performance as well as to document measurement uncertainty.

2.2.1 Thermal Test Board

The test vehicle contains three main parts: chip, substrate and test board. The chip used in the test board is a passivation test (PST) thermal chip provided by Delphi. The footprint of a basic cell is 6.35 mm x 6.35 mm however, to increase the chip size, a 2 x 2 array of basic chips is used in the test vehicle to form a 12.7 mm x 12.7 mm chip surface area. The basic thermal test chip contains two main elements: diode and resistor. The diode is used for sensing the current and allows on-die temperature monitoring, while the resistor is the heating element of the chip. Figure 14 shows the thermal test chip connected to the Agilent DC power supply (Model 6644A) and precision resistor, while the diodes are connected to the Keithley 2400 sourcemeter. The voltage readings are recorded with the Agilent data acquisition (Model 34970A) system. All four resistors

(18 ? each) connected in series give a total heating resistance, R_T, of 72 ? and each diode has a forward-biased voltage value of 3.556 ? 0.001 V at 25 ?C ambient temperature.

The junction temperature of the chip is monitored through all experiments by recording the diode voltage. To determine the relationship between the voltage drop across the diode and the junction temperature of the chip, a constant current source of 1 mA is supplied to the chip in a temperature-controlled environment and the voltage values are recorded. During this calibration process it is not necessary to supply heating power to the chip since the voltage drop across the diode is dependent on both the current flowing through the diode and the temperature of the diode which is determined by the oven temperature. Intel Corporation uses similar technology to determine the operating temperature of its processors [19].

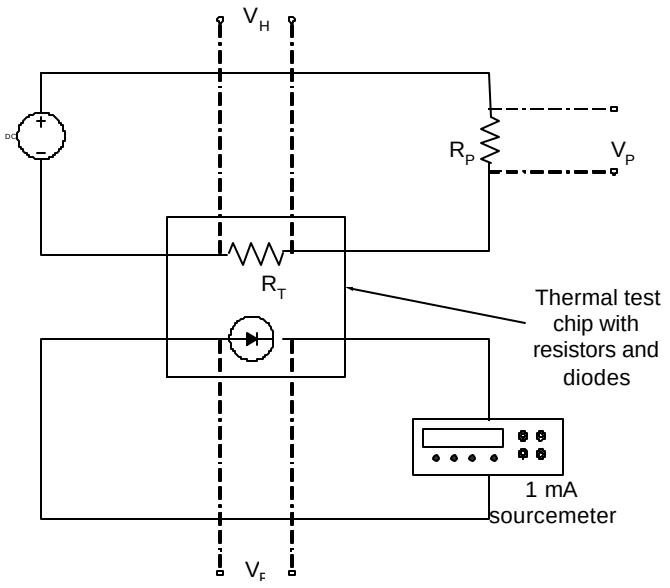

Figure 14 Thermal test chip connection with measured voltages

Figure 15 shows a schematic of the set-up and details of the step-by-step calibration process are listed below:

1. Test all 4 diodes at room temperature with sourcemeter. Diode voltage ? 3.556 V
2. Test resistors with multimeter. Average resistance value is 18 ? .
3. Connect four resistors in series.
4. Place assembled test board into temperature-controlled environment (oven) at room temperature.
5. Supply constant current of 1 mA with Keithley 2400 Sourcemeter to each diode.
6. Allow steady state voltage (? 0.001 V)
7. Record diode voltage from 2400 Sourcemeter at 5 minute intervals
8. Heat oven to 50?C and allow steady state temperature
9. Repeat step (7)
10. Repeat steps (8) and (9) in 25?C increments to a maximum of 100?C

Figure 16 shows the relationship between the diode voltage and chip temperature determined from the calibration data. Since all four diodes are identical, it is only necessary to monitor two diodes during the experiments. This linear relationship is used throughout the experiments to determine the chip's junction temperature by recording the voltage as the chip is heated. For instance, if the diode voltage is measured as 3.451V at a known chip power of 5 W, then using the equation for diode 1 from the calibration curve (Figure 16), the junction temperature, T_j, is calculated to be 38.9 ?C.

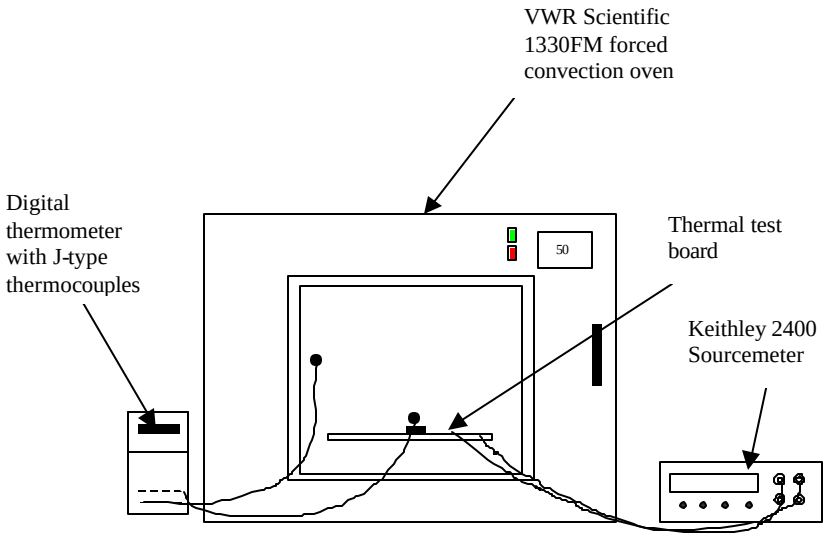

Figure 15 Schematic of calibration procedure for thermal test boards

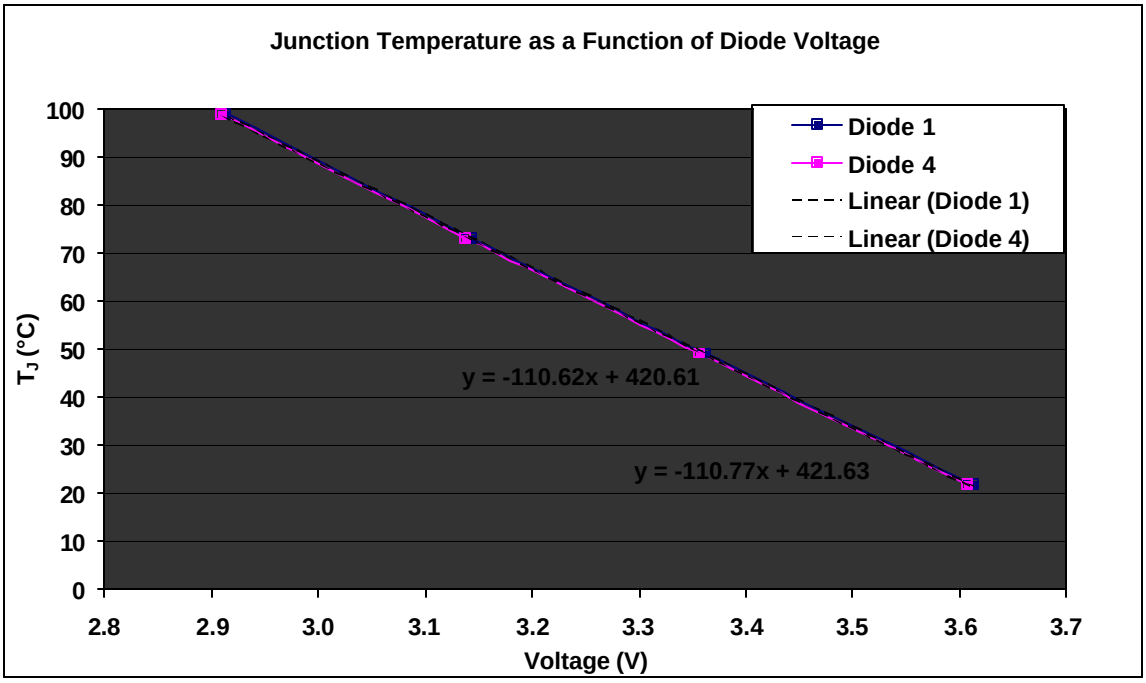

Figure 16 Calibration results for thermal test chip

2.2.2 T-Type Thermocouples

Temperature is measured at various locations in the cooling system with T-type thermocouples, which are connected to the data acquisition system. All thermocouples were external and kept in place with hardened epoxy; one thermocouple was placed at the external top wall of the evaporator ($T_{evap\ wall}$), while three thermocouples were placed at each condenser inlet and outlet tube. The thermocouples were calibrated against a precision mercury thermometer in an ice-water (0 ?C reference points) mixture to an uncertainty of ? 0.7 ?C.

2.3 Experimental Procedure

An experimental procedure was developed to test the thermal performance of the two-phase system and also to study the effects of design parameters on the total power dissipation. First, it is necessary to ensure a leak proof system when a closed-loop cooling solution (with liquid) is applied for electronics. The metallic evaporator and condenser prototypes were joined with clear Tygon R-3603 lab tubing to permit flexibility and visibility. The tubing with inner diameter of 3.175 mm was fitted over the inlets and outlets of the two metallic components (D_o = 3.175mm), and a high temperature epoxy adhesive (Loctite E-120HP) sealed the overlapping edges. Tee fittings were included in the loop to provide inlet and outlet ports for the evacuation and filling process, while mini brass ball valves (vacuum rating: 29 in-Hg) closed the system. Prior to the experiments, the dielectric liquid PF5060 (perfluorocarbon) was vigorously boiled for 45 minutes after which the flask was sealed and the fluid cooled. This

degassing procedure minimizes the amount of air dissolved in the fluid to ensure a saturated liquid-vapor closed system.

An evacuation and back filling process, similar to that used for heat pipes, is used in the first critical step. Valve 1 is closed and the system is evacuated through valve 2 to a sub-atmospheric pressure measured with a TIF digital pressure gauge (? 2% of reading). The absolute system pressure is typically 2 kPa ? 1 after the initial evacuation. Valve 2 is then closed and valve 1 is opened partially to fill the system with a measured amount of working fluid from the burette, during which the system pressure increases slightly but still remains below atmospheric pressure. The system is briefly evacuated again (if necessary) to start the experiment at a specific initial system pressure. An extra amount of working fluid is added during the filling process to compensate for the re-evacuation. At this point the system is an isolated partially filled closed-loop sub-atmospheric system. When all the components are in place, the fans are turned on and data recording begins at steady state room temperature.

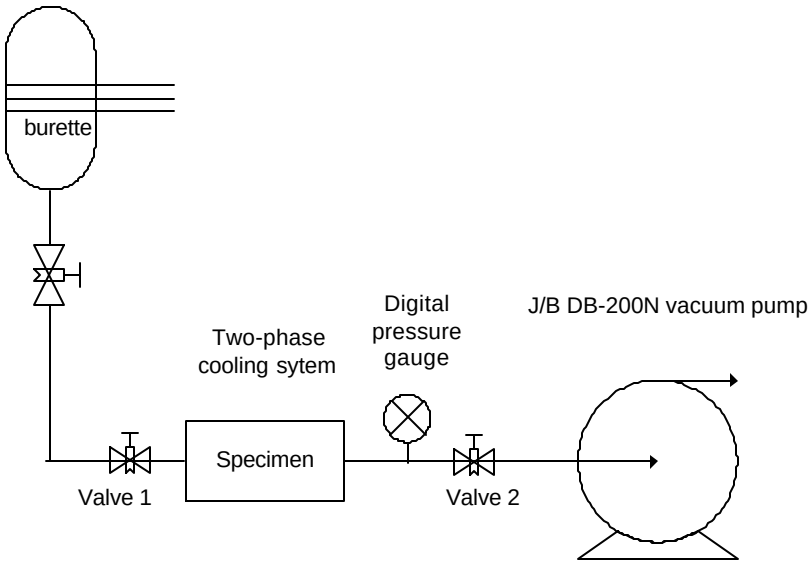

Figure 17 Schematic of evacuation-filling procedure for closed loop system

2.3.1 Degassing of Dielectric Liquids

Dielectric liquids are the chosen coolants for electronic thermal management systems because of their high dielectric strength, low dielectric constant, and chemical inertness. These characteristics of fluorochemical fluids are especially desirable for immersion liquid cooling where component heat fluxes in excess of 10 W/cm^2 can be removed with saturated pool boiling. However, the perfluorocarbons, made by 3M Inc., also have relatively low critical pressures, thermal conductivities and specific heats, and very large air solubility. Tests with perfluorocarbons have shown air solubility of 40-50% by volume at atmospheric conditions, compared to 2% by volume for water [20].

A degassing procedure is necessary to eliminate the non-condensable air from the working fluid and improve the system's efficiency. The solubility of air in a refrigerant's liquid phase is much lower compared to the perfluorocarbons and air is not significant as a liquid phase contaminant [21]. According to ARI Standard 700, virgin refrigerant or

reclaimed R12 must contain ? 1.5% air or non-condensable gases by volume, and no more than 0.5% other refrigerants, by weight. APPENDIX E shows characteristics of some refrigerants with the low value of 1.5% non-condensable by volume.

For a liquid cooled system the fluid can be selected from fully fluorinated fluorocarbons (FC-72, -75, -87), chlorinated fluorocarbon (R-113) or water. Water is the superior fluid based on its thermophysical properties, however the chemical inertness of the FC liquids make them the safe choice for electronics thermal management. Chlorinated fluorocarbon, R-113, is found to offer better heat removal capability than the FC liquids due to its lower percentage of non-condensables [22]. Impurities in the fluid can result in trapped air inside a system and significantly reduce the system's efficiency. To limit this problem the fluids are degassed prior to any experiments and extra care must be taken to eliminate the introduction of air during the transfer to the system or storage tanks. In the current study, air measurements are not recorded, however based on the data referenced above it is assumed that trapped air in the working fluid (PF5060) is 40 – 50 % by volume.

2.3.2 Data Acquisition

A data acquisition system is utilized to collect data from which the total heat dissipation from the test chip can be calculated. An Agilent DC power supply (Model 6644A) provides voltage to the heating resistors, R_H, which is connected in series to a 1? precision resistor, R_P. A data acquisition switch unit (Agilent 34970A) with a 20-channel multiplexer module allows measured values to be assigned to individual channels. The

voltages, V_H and V_P, are measured across the total heating resistance and 1? precision resistor respectively. The actual heating current, I_H, and heating power, P_H are found from the equations below.

$$I_H \; ? \; \frac{V_P}{R_P} \qquad\qquad P_H \; ? \; I_H \; ? V_H$$

The Keithley 2400 sourcemeter is turned on to supply a constant current (1 mA) to the diode and the fan is set at constant flow rate. Steady state readings are taken for the chip without any heat input at room temperature after which heat is supplied in 5 W increments. During the experiment the input power is incrementally increased and temperatures are recorded until the system sustains steady state for at least 30 minutes. The junction temperature and heating power are calculated form the recorded temperature and voltage values. The two-phase cooling system's performance is determined by the total power dissipation when the chip is at the maximum junction temperature (95 ?C).

2.3.2 Uncertainty Analysis

The system's performance was characterized by the test chip's junction temperature value at specific chip powers. These calculated values involve measured quantities: temperature and voltage. The accuracy of the instruments used in reading those quantities varies; therefore the uncertainty involved in calculating the power will be a function of the accuracy of the instruments. The uncertainty can be determined in quantitative terms by using uncertainty analysis. If an indirect measurement (y) is a function of N direct measurements, the method of Kline and McClintock states that the uncertainty (u) is expressed as:

$$u^2 = \left(\frac{\partial y}{\partial x_1}u_1\right)^2 + \left(\frac{\partial y}{\partial x_2}u_2\right)^2 + \ldots + \left(\frac{\partial y}{\partial x_N}u_N\right)^2$$

Applying the general formula to a more specific case relevant to this study and using regression analysis, the uncertainty for thermal chip power, P, is ± 1.2 W (0 < P < 30W).

$$P = VI$$
$$u_p^2 = u_{p\_V}^2 + u_{p\_I}^2$$
$$u_p^2 = \left(\frac{\partial P}{\partial V}u_V\right)^2 + \left(\frac{\partial P}{\partial I}u_I\right)^2$$
$$u_p^2 = \left(\frac{P}{V}u_V\right)^2 + \left(\frac{P}{I}u_V\right)^2$$

where;

P = Power

V = Voltage

I = Current

u = Uncertainty

The independent variables for the heat transfer experiments in this study are temperature, and voltage. The uncertainty in the T-type thermocouples was found to be ± 0.7 °C from the calibration process. The uncertainty in the junction temperature (T_J) of the thermal test chip depends on the uncertainty values found in the calibration process, as well as the data acquisition system. An uncertainty value of ± 0.9 °C is calculated for the junction temperature of the thermal test chip. The uncertainty in the DC voltage measurement from the data acquisition system was specified by the manufacturer as ± (% of reading + % of range). In the current case the maximum range is 10 V for the diodes, therefore the measured accuracy for the diode is ± (0.0015% of reading + 0.0004% * 10).

The precision resistor used to measure the heating current was accurate to ? 1%. The manufacturer specifies a digital accuracy of ? (2% of reading) for the pressure gauge for a range of 0 – 101 kPa.

CHAPTER III

COMPUTATIONAL ANALYSIS

The total rate of heat transfer from the condenser to the ambient air was estimated using the correlation for a stack of parallel plates cooled by laminar forced convection [23]. Initial analysis showed the feasibility of dissipating the required heat (30 W) in the specified condenser volume (160 x 55 x 25 mm) and also gave an approximate value for the optimum plate spacing for maximum heat transfer rate.

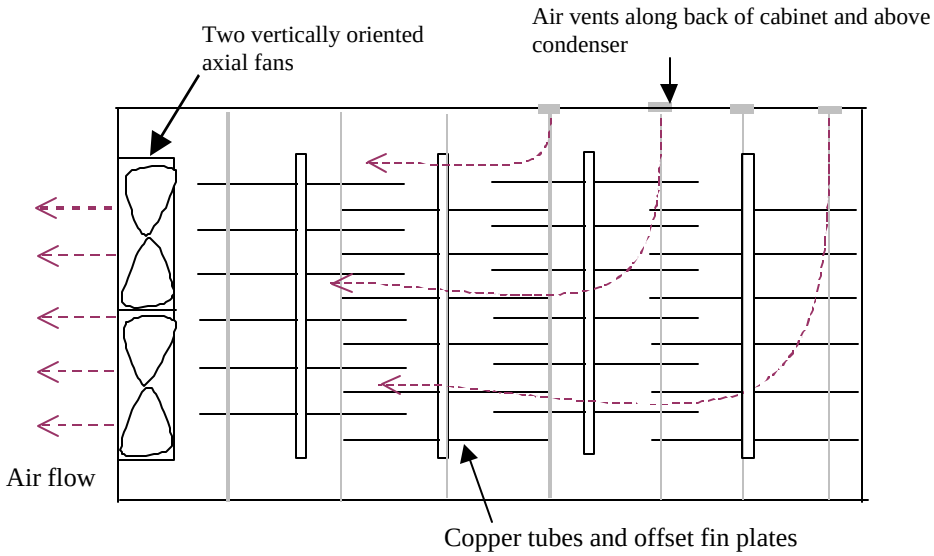

Figure 18 Top view of Design 1: offset fins and vertical fans

Two design concepts for the condenser system were evaluated using computational modeling; Figure 18 shows Design 1 in which plate fins are offset by 3 mm along a serpentine tube, while vertically oriented fans provide forced convection over the fins. Since heat transfer is inversely proportional to boundary layer thickness, the offset fins present the advantage of disrupting the growing boundary layer, thus

increasing the heat transfer from the fins. The disadvantage of this design is the increased pressure drop across the condenser. The fins are attached to copper tubes, which allow continuous flow by joining the straight tubes with u-shaped tubes (not shown). Ventilation is positioned along the back to force air flow over the path of more resistance.

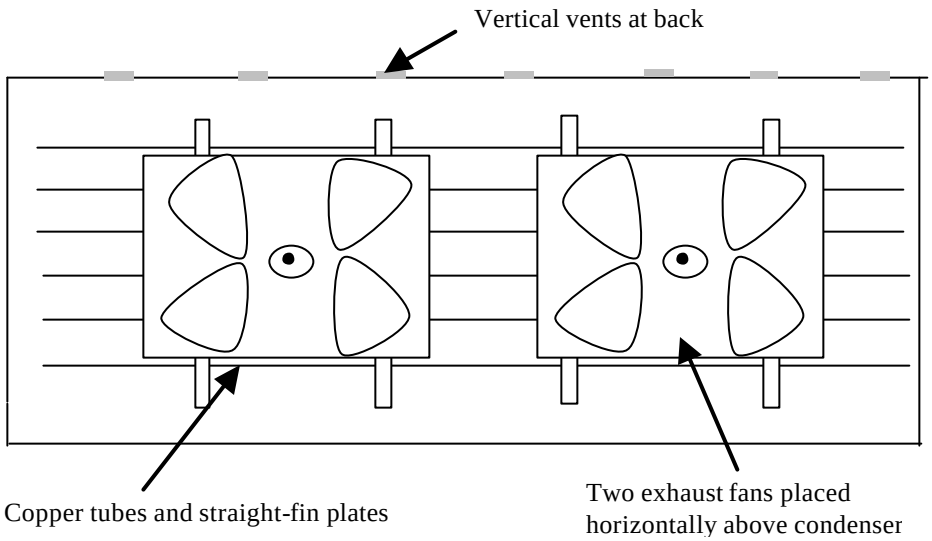

Figure 19 Top view of condenser design 2

An alternative design for the condenser, Figure 19, also uses forced convection in a different configuration. The parallel plates are straight with more powerful fans placed horizontally. Vents are placed along the length of the condenser at the back of the cabinet. Although this concept employs fans with 40% higher flow rate, there is a lack of additional ventilation as well as limited vertical height for the plate fins. Both designs use simple straight fin plates for easy manufacturability and reduced cost.

Commercial software, Icepak 3.2, was used to simulate both design concepts. Figure 20 shows the full laptop model containing the condenser system in addition to

other components placed in the specified dimensions of the laptop cabinet, however the analysis was focused on the shaded area immediately surrounding the condenser. The saturation temperature at 1atm is applied to the copper tubes as the thermal boundary condition, and the thermal properties of copper are assigned to the tubes and fins. Design 1 is simulated with vertical fans of two sizes, 20 x 20 x 10 mm and 25 x 25 x 10 mm, due to the height constraint of the laptop cabinet. This constraint also places restriction on the fan's thickness in design 2 in which the horizontal fans each have dimensions of 40 x 40 x 6 mm thick. Table 2 summarizes the boundary conditions and results for both designs showing a 47% increase in heat dissipation for design 1. The serpentine off-set fin-tube condenser is selected for fabrication and evaluation.

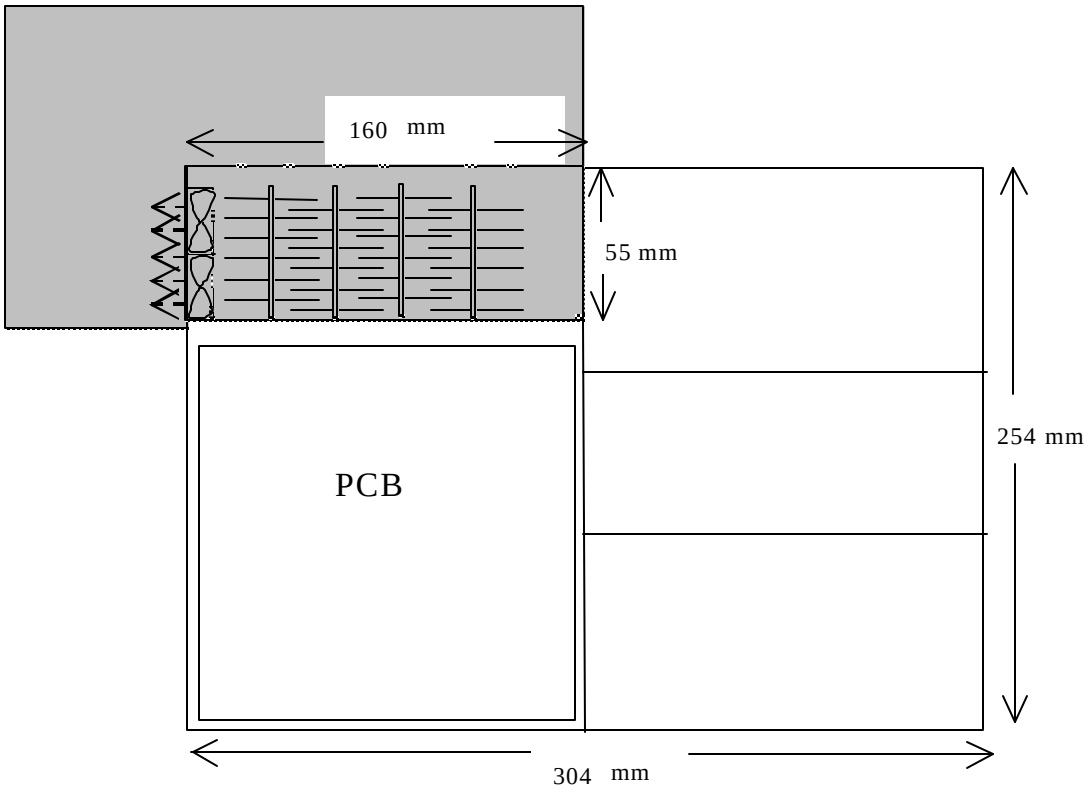

Figure 20 Top view of laptop cabinet showing shaded area for computational analysis

Table 2 Computational analysis of condenser designs 1 and 2

Thermal boundary conditions: T_{tube}= 60?C, $T_{?}$ = 25?C, P_{atm}= 101 kPa (1 atm)		
	Design -1	**Design -2**
Fan details	DC Brushless fans: max flow rate: 0.0017 m^3/s (3.5 CFM), static press: 62.3 Pa (0.25 inch-H_2O)	DC Brushless fans: max flow rate: 0.0026 m^3/s (5.5 CFM), static press: 25 Pa (0.1 inch-H_2O)
Geometric description	25 x 25 x 10 mm	40 x 40 x 6 mm
Maximum power dissipation	32 W	17 W
Air Flow	0.0024 m^3/s (5.1 CFM)	0.002 m^3/s (4.0 CFM)

3.2 Numerical Analysis

The air-side heat removal from the condenser model (design 1) is further analyzed with Fluent 6.2. The Fluent model with identical fan curves, material properties, and boundary conditions gave a maximum power dissipation of 24.9 W compared to 32 W from the Icepak model (Table 2). The Icepak simulations were done to show the feasibility of heat transfer from the condenser, however the Fluent model was based on the actual prototype which had been fabricated. Although the dimensions, material properties, and boundary conditions in both models were similar, there was a difference in the modeling of the vents. Current laptop computers were used to estimate a free area ratio coefficient (open vent area/total vent area) which was applied to the Icepak models, compared to the Fluent model which eliminated the need for a coefficient and simply modeled each individual vent based on the dimensions of the prototype. This change between the Icepak and Fluent models can account for the difference in maximum power dissipation results.

A 3D model for the condenser was built with the four hollow tubes and attached thin plate fins in an enclosure with individually modeled vents. The physical dimensions were identical to the actual prototype, thermal boundary conditions were applied to the tubes, and appropriate material properties were assigned to each component. The operating pressure was set at atmospheric pressure while no gravity was applied since it was a forced convection model. The inlet vents were modeled as simple pressure inlets while a polynomial profile for the exhaust fans gave the pressure jump in terms of normal velocity. Each fin was coupled with the copper tubes and shell conduction was enabled

to compute the conduction across the fins. Global boundary conditions include stationary walls, no slip shear conditions on walls and steady state conditions for all simulations. The grid was a hexahedral/wedge cell combination with a total of ? 220,000 cells. Although the model was not complex, care was taken to mesh the volumes individually to prevent errors in the grid generation. The converged solutions were tested to show grid independence as well as convergence criteria independence by finding the numerical values only differ by 1-2 %. Details on the grid include:

Domain Extents:

x-coordinate: min (m) = 0.0, max (m) = 1.6e-01

y-coordinate: min (m) = 0.0, max (m) = 5.5e-02

z-coordinate: min (m) = 0.0, max (m) = 2.3e-02

Volume statistics:

minimum volume (m^3): 1.04e-10

maximum volume (m^3): 1.68e-09

total volume (m^3): 2.01e-04

Face area statistics:

minimum face area (m^2): 4.16e-07

maximum face area (m^2): 1.92e-06

Numerical analysis is used to examine the effect of air flow and vent location on the condenser's ability to reject heat to ambient air. There are many limiting factors such as size, volumetric flow rate and acoustic noise, which influence the fan selection to

provide the forced air flow over the condenser. The performance curves for the two 25 x 25 x 10 mm fans used in the experiments and numerical simulations show a maximum static pressure of 62.3 Pa (0.25 in-H_2O) and volumetric flow rates of 0.0017 m^3/s (3.5 CFM). Forced convection heat transfer from the condenser can be further enhanced by increasing the air flow across the system or by maximizing the air flow from the fans already employed in the cooling system.

Two models with identical boundary conditions show the difference in velocity profiles and heat transfer rate when 25% of the openings (vents) nearest to the fan are closed, thereby forcing more air flow through the condenser. Figure 21a shows the top view of the velocity profile in the z mid-plane with all vents open compared to Figure 21b with vents nearest to the fan closed off. Although the maximum velocity is 4.8 m/s in both models, the velocity vectors show the difference in flow patterns near the fans (identified by points 1 & 3 on Figure 21) where in the first scenario the majority of air flows through the vent nearest to the fans and exits the enclosure; while the second scenario shows a more distributed flow through the first two rows of fins. In both cases, the pressure drop across the condenser is large and the cooler end of the condenser (points 2 & 4) do not benefit from the forced convection or the nearby vents.

Figure 22 shows the corresponding front view of the temperature distribution in the enclosure. In general, the base of the enclosure maintains a higher temperature since the vents are at the top and tubes near to the fans can be as much as 30 ?C cooler than the condenser outlet tubes. With more efficient use of the vents, the air is ducted through the plate fins (more resistive path) and dissipates 31 W which is a 20% increase over the

original 25 W. Figure 21 and Figure 22 illustrate the stagnant air in the enclosure as well as the high temperature air at the furthest points from the fans. A change in vent location can assist air flow through the condenser and improve the efficiency and overall heat transfer of the system.

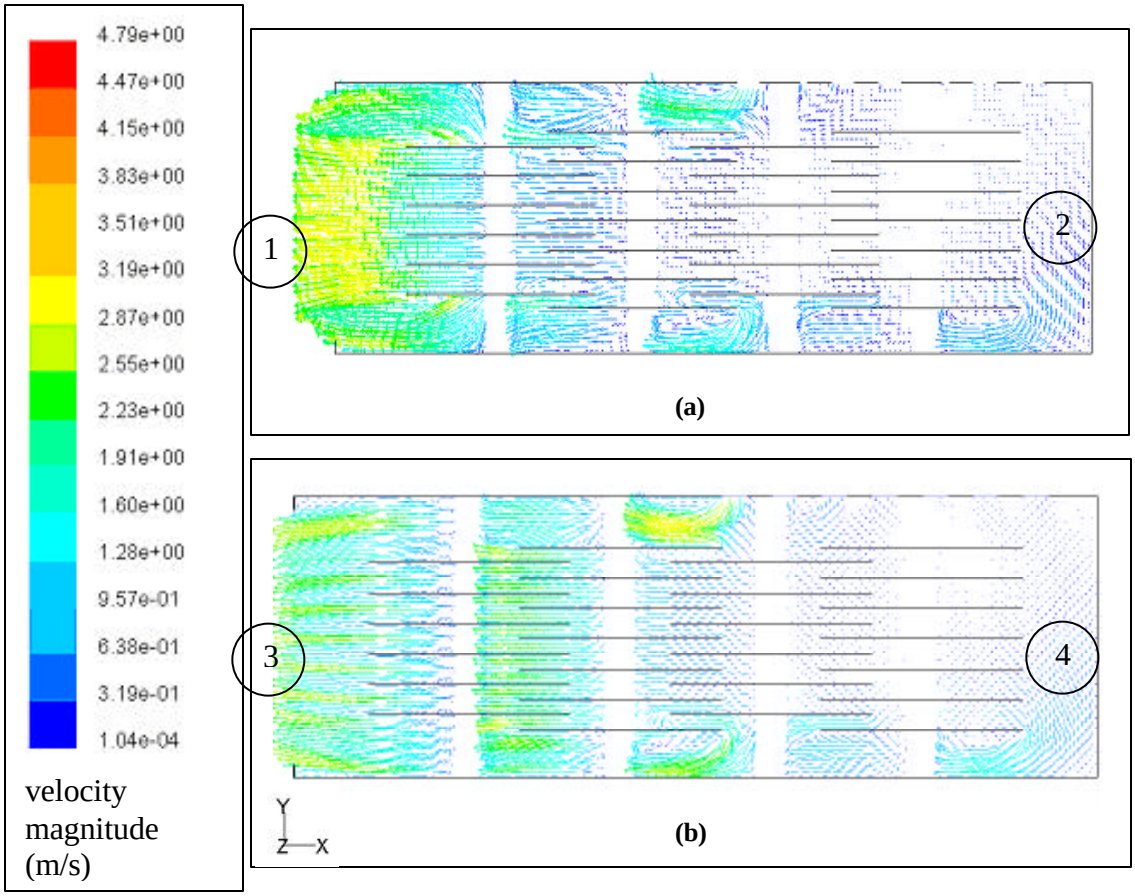

Figure 21 a & b Top view of velocity profiles showing effects of ventilation in z mid-plane

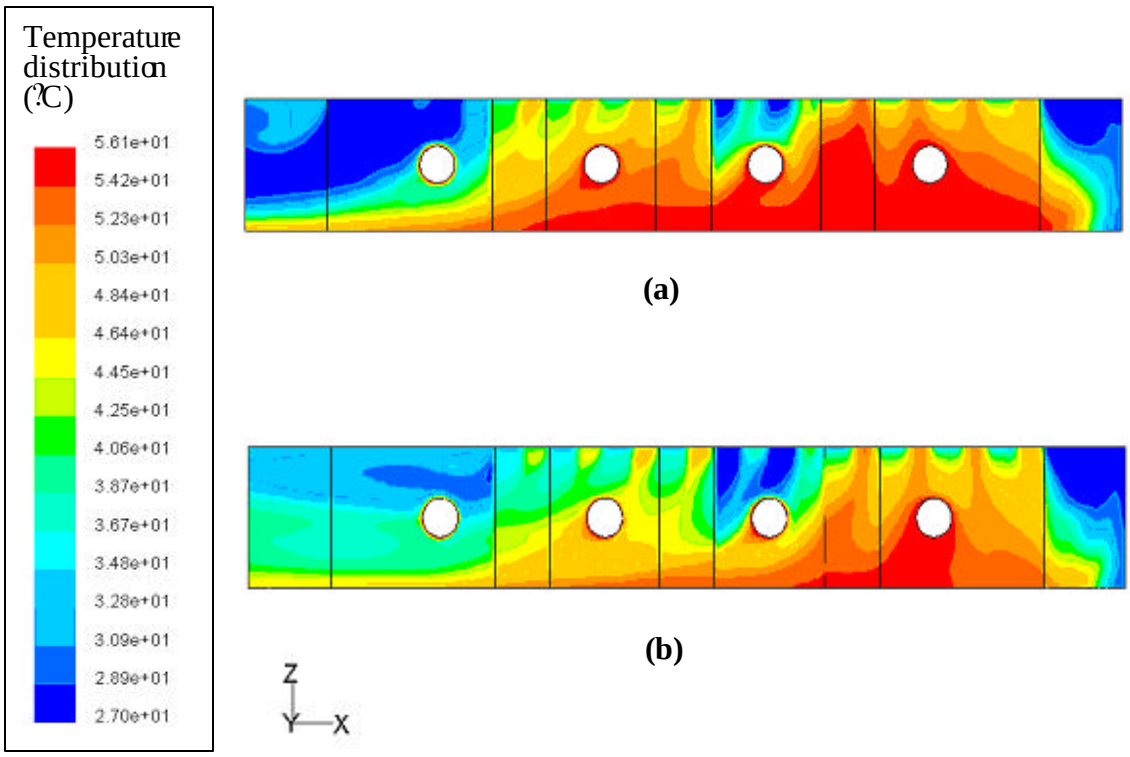

Figure 22 Front view of temperature distribution in y mid-plane

The saturation temperature (56 ?C) for PF5060 at room temperature was applied at the thermal boundary condition to the tubes for the computational model, which would be the ideal case. However, the experiment data shows an average tube temperature of 35 ?C for the condenser with a maximum power dissipation of 25 W from the entire cooling system. This boundary condition was then used in the computations to determine the heat dissipation from the condenser with low temperature tubes (35 ?C). The temperature distribution (Figure 23 and Figure 24) was identical in both models since the air flow was provided by the same fans, however the heat transfer from the 35 ?C condenser was found to be 6 W.

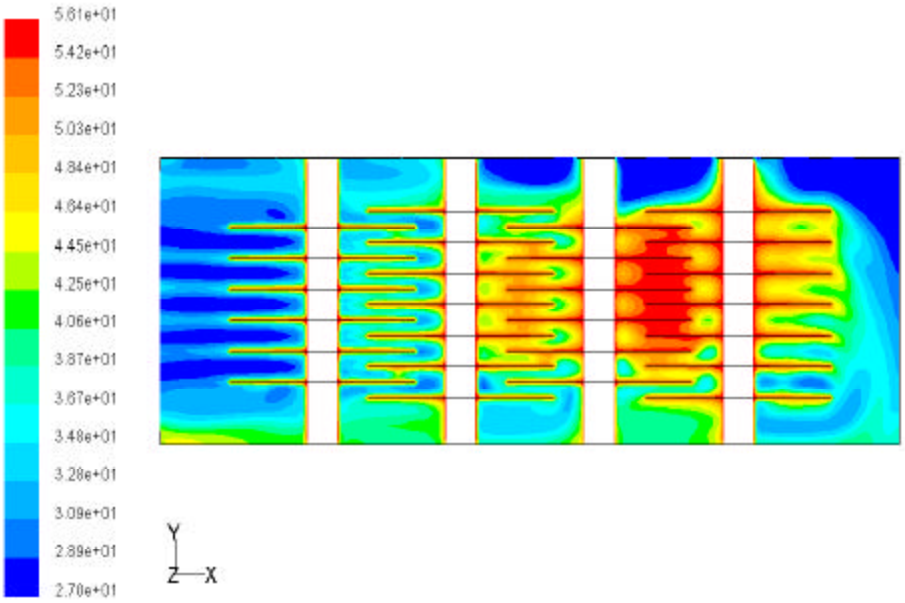

Figure 23 Top view of temperature distribution in the z mid plane

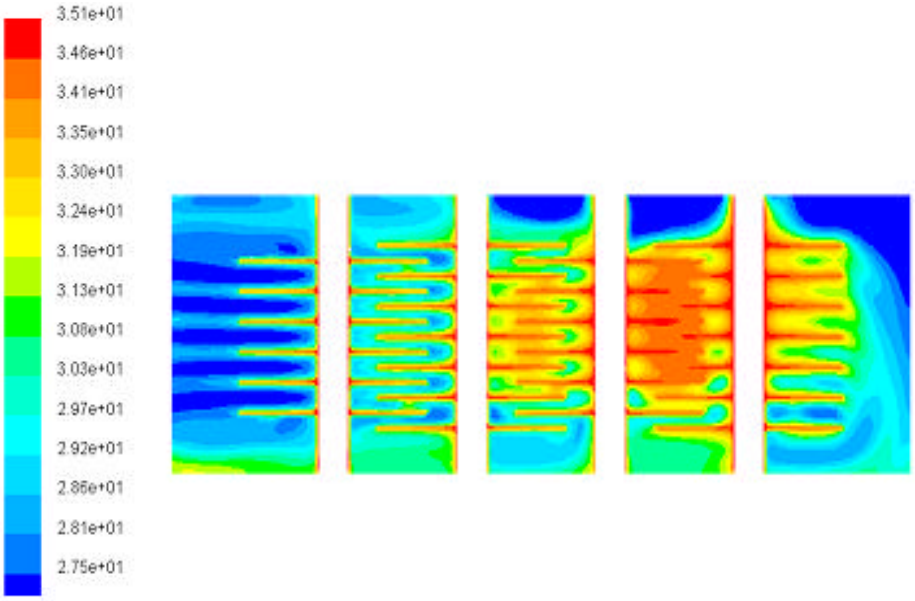

Figure 24 Top view of temperature distribution (z mid-plane) for low temperature tubes

Phase transition from saturated vapor to saturated liquid occurs in the condenser; therefore the forced air convection over the tubes and plate fins can limit the total heat transfer rate. A closer examination of the velocity profiles inside the enclosure provides more insight to the flow patterns and flow impedance. Figure 25 shows a clearer view of individual velocity vectors. These figures confirm the air flow along the paths of least resistance and not through the plate fins. Figure 26 zooms in on the tube nearest to the fans and shows the velocity vectors in the y mid-plane. The upper half of Figure 26 (at the top vents) experiences some re-circulatory flow and the air exits at higher velocity near the bottom wall of the enclosure.

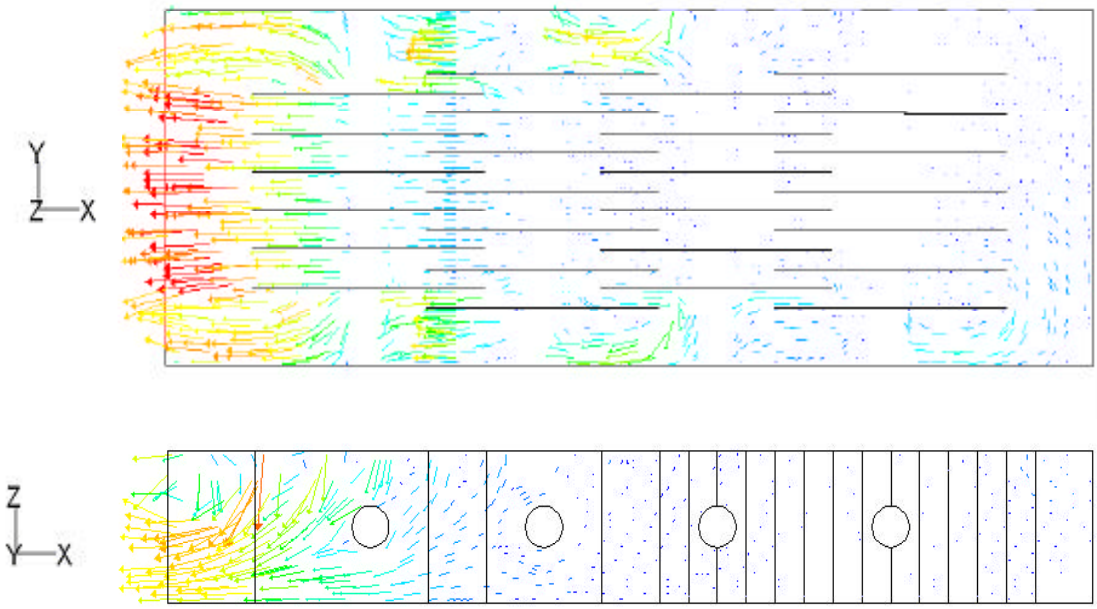

Figure 25 Top and front views of global air flow across the condenser

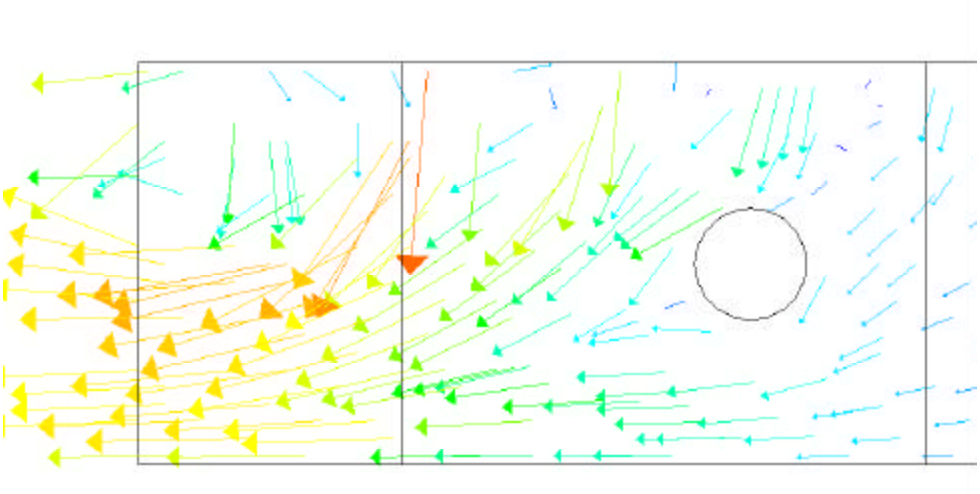

Figure 26 Zoom-in of front view showing flow entering from the top vents

CHAPTER IV

OPERATING PARAMETERS AND THEIR EFFECTS ON THE THERMAL PERFORMANCE OF THE TWO-PHASE COOLING SYSTEM

Heat transfer results are presented in the previous chapter for the air-side analysis of the condenser. An experimental study was carried out to determine the overall heat transfer characteristics of the two-phase cooling loop. Experimental results presented in this chapter illustrate the viability of implementing a compact two-phase cooling system in a laptop computer. A gravity-driven loop was first tested to determine the limits of the system, after which a pump was incorporated to assist liquid flow back to the evaporator. The cooling system's performance is evaluated by varying parameters such as the volume fill ratio of coolant, initial system pressure, pump flow rate and heat input.

4.1 Baseline Configuraton of Two-Phase Closed Loop

The baseline configuration seen in Figure 8 consists of the metallic evaporator and serpentine fin-tube condenser joined with flexible Tygon tubing. The heat to the evaporator cavity is incrementally increased causing increased vapor generation. In this gravity-driven system the condensate return must provide continuous circulation of liquid to the evaporator. Data in Figure 27 shows high thermal resistance values for the gravity-driven loop in the range of 10 – 12 ?C/W at very low heat fluxes. The system flow resistance and condenser performance limit the condensate formation and the pressure in the loop increases until some equilibrium state is attained.

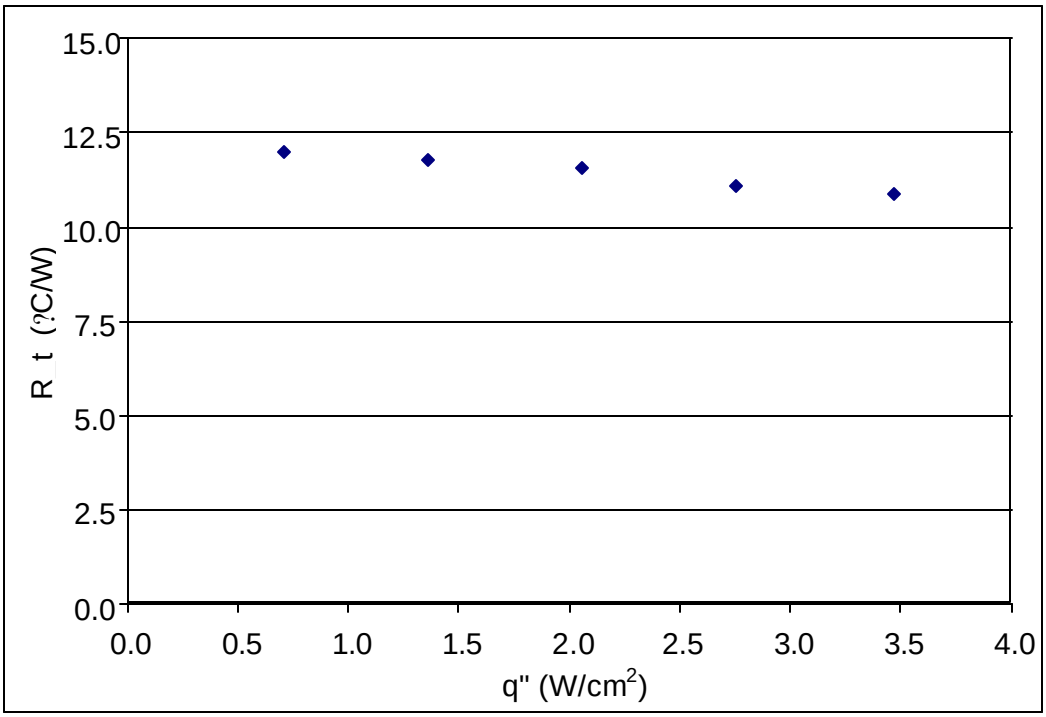

Figure 27 Peformance of thermosyphon loop without pump assitance

The initial system pressure is 50 kPa (T_{sat}=40 ?C), and heat is supplied in 1-W increments for a range 1 – 6 W. Boiling is observed first from the evaporator outlet and then from both inlet and outlet of the evaporator since a flow pattern is not established. The chip temperature continuously rises as the heat input is increased and boiling is no longer observed at 3.5 W/cm^2. The large flow resistance at the condenser inlet prevents any circulation of vapor and liquid; resulting in a localized two phase process in the evaporator section of the loop. Figure 28 shows the steady increase in chip temperature as well as the constant inlet and outlet temperatures of the condenser all relative to the ambient temperature. The negligible increase in condenser temperatures indicates the

large pressure drop in the system which inhibits any condensate formation in the condenser.

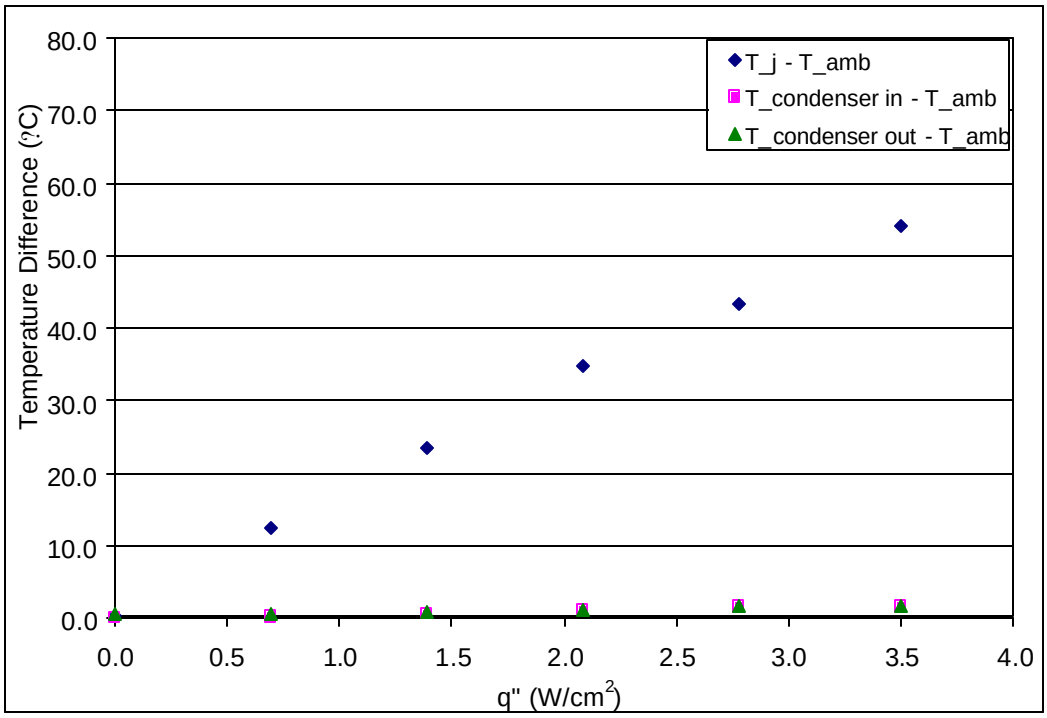

Figure 28 Temperature differences of chip and condenser in gravity-driven loop

4.2 Parametric Study

Based on the data for the gravity-driven compact two-phase system, it is evident that flow assistance is required to overcome the pressure drop in the condenser. A variable-speed drive Masterflex pump is implemented on the return liquid side of the loop (Figure 29) to assist liquid flow back into the evaporator. The pump is used for all experiments in the parametric study with a steady flow rate of 0.033cm^3/s (2 ml/min).

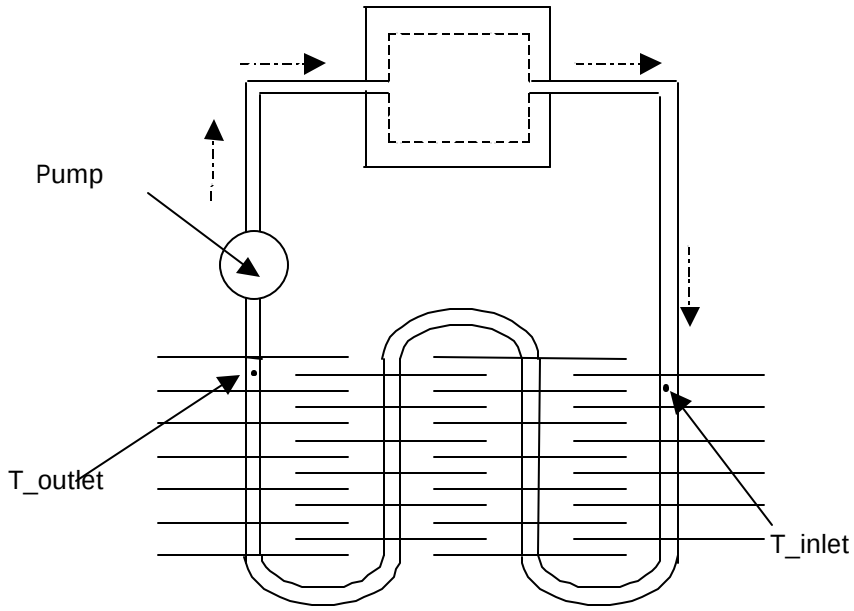

Figure 29 Schematic of two-phase closed loop with pump

4.2.1 Effect of Working Fluid Fill Ratio

The principle of this liquid cooling system is to take advantage of the significant latent heat effects associated with phase change; therefore the amount of working fluid is an important parameter affecting the performance and cost of the two-phase cooling system. It is necessary to charge the system with a sufficient amount of liquid to prevent dry out at higher heat fluxes. In larger systems, the working fluid is fully contained in the evaporator cavity, however this compact system requires more fluid than the capacity of the small evaporator. The fluid partially fills the evaporator and also a portion of the connecting tubes to the condenser. Experiments were conducted for fill ratios (volume of fluid/volume of closed loop) of 25%, 50% and 75%.

A fill ratio of 25% (5.0 ? 0.1 cm^3 PF5060) shows initial decrease in thermal resistance as boiling begins, but when the heat flux approaches 9 W/cm^2 the amount of

liquid diminishes rapidly as the condensate is not formed quickly enough to return to the evaporator. The performance was noticeably better for higher fill ratios where some amount of working fluid was consistently visible in the connecting tubes throughout the experiment compared to the dry-out that occurred with 25% fill. In a liquid cooled system there is an optimum volume of liquid as shown by both fill ratios 50% and 75%, where there was only a 0.1 ?C/W difference in thermal resistance for a 10.5 W/cm^2 maximum achievable heat flux. It is difficult to ensure complete accuracy with the evacuation-filling procedure for this two-phase system, and this difficulty level increases with larger volumes of working fluid as well as lower initial system pressure. The cost of the PF5060 working fluid was also considered and all future experiments were conducted with a 50% fill ratio which is the lower end of the optimum range of liquid fill volume.

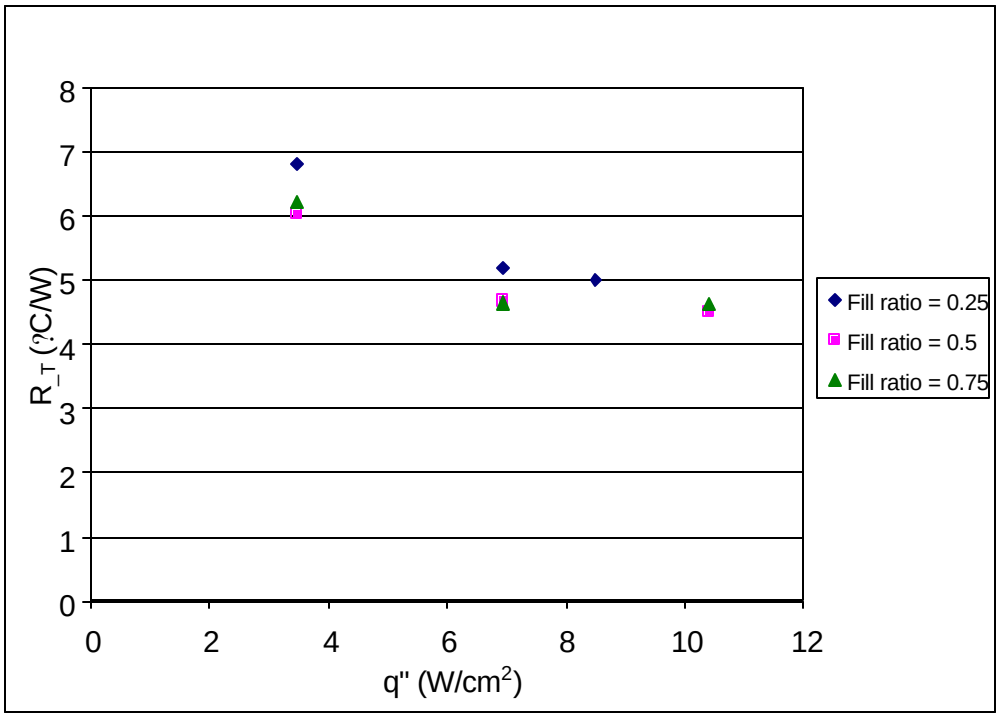

Figure 30 Effect of working fluid volume fill ratio on thermal performance of system

4.2.2 Effect of Initial System Pressure

The internal pressure of a closed loop system is an important parameter affecting the boiling process in the two-phase system. Properties of the working fluid, PF5060, such as a boiling point of 56 ?C at 1 atm and a low latent heat of vaporization, h_{fg}, of approximately 92 kJ/kg affect the onset of boiling in the evaporator and convection forces to begin transferring heat away from the heat source. Three values of initial system pressure were studied and its effects on thermal performance are shown in Figure 31. The working fluid's low saturation temperature at atmospheric pressure implies even lower boiling temperatures under vacuum conditions; however during the phase change the internal pressure also increases which raises the saturation temperature of the fluid in the evaporator.

Experiment results show that an equilibrium saturated vapor-liquid state is achieved and the chip maintains its steady state temperature until the heat flux is increased. Figure 31 shows the effect of initial system pressure on the overall thermal resistance. An initial system pressure of 30 kPa gives the best performance with an 80% decrease in the minimum thermal resistance compared to an initial pressure of 70 kPa. The advantage of a low initial pressure in a closed system seems more evident at higher heat fluxes where there is a 0.4 ?C/W difference in thermal resistance values between 50 kPa and 70 kPa. A more technical and systematic evacuation and filling procedure were beyond the capability of available equipment, however it is apparent that the system's performance depends greatly on the initial system pressure. Boiling is initiated at lower

temperatures in a sub-atmospheric system and the heat transfer process begins long in advance of chip's temperature limit.

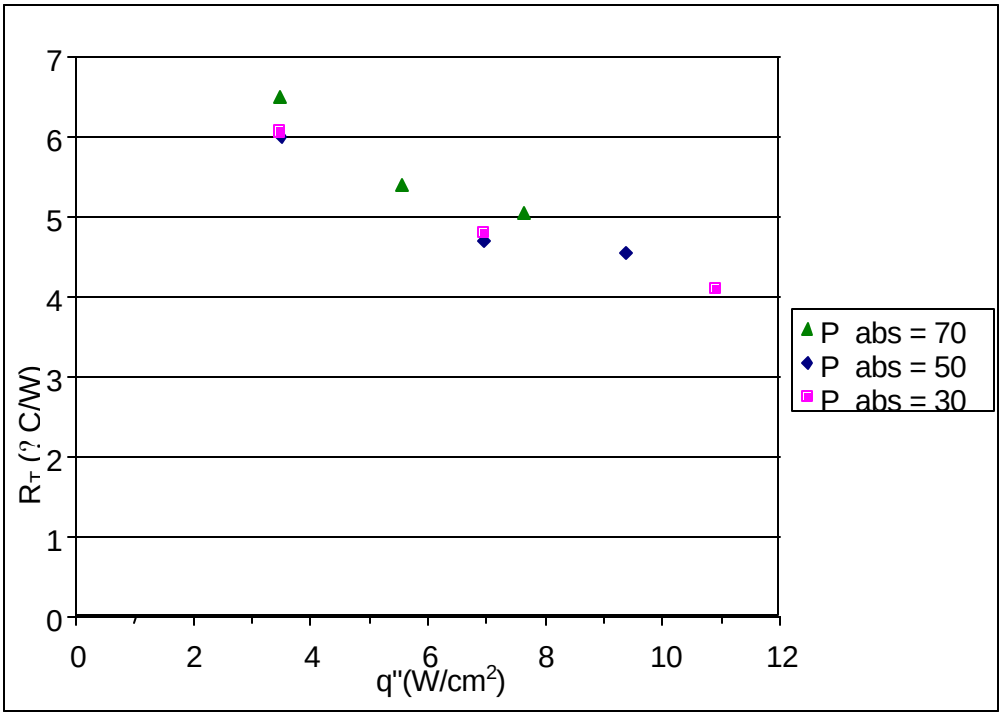

Figure 31 Effect of initial system pressure on two-phase closed loop

4.2.3 Effect of Pump Flow Rate

It was established in section 4.1 that assisted forced convection was required to overcome the large internal pressure drop of the condenser. A pump was implemented on the liquid return side of the evaporator (Figure 29) and the experiments repeated so far have been conducted with a constant pump flow rate of 0.033 cm^3/s (2 ml/min). Now the liquid flow rate is varied in $0.017 cm^3/s$ (1 ml/min) increments while the optimum parameters from prior experiments are applied as constant values. Total thermal resistance values are reported in Figure 32 for pump flow rate range of 0.033 cm^3/s (2

ml/min) to 0.1 cm^3/s (6 ml/min). An induced flow through the system also allows the condenser to perform more efficiently which can be seen in the average condenser temperatures shown in Figure 33.

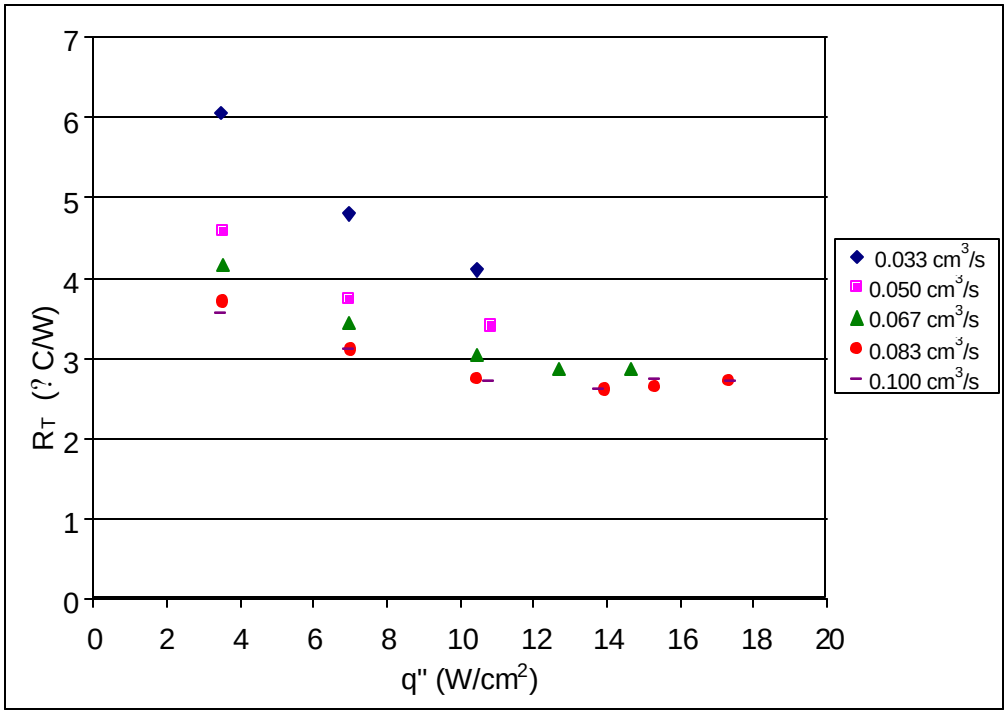

Figure 32 Effect of pump flow rate on two-phase closed loop system

A higher pump flow rate enhances the heat transfer from the condenser and reduces the total thermal resistance of the system. The serpentine condenser provides larger surface area for external forced convection, however it also restricts the flow through the small longer internal condenser path from inlet (saturated vapor) to outlet (saturate liquid). At low flow rates the condenser maintained an approximate room temperature, then with higher forced convection a temperature difference developed across the condenser. Figure 32 shows the overall thermal resistance of the closed loop system approaching its limit at pump flow rate 0.08 – 0.1 cm^3/s (5 – 6 ml/min).

Additionally, the maximum average condenser temperatures recorded (Figure 33) are below the saturation temperature of PF5060 under the specified conditions. Ideally the condenser inlet temperature should be the same as the saturation temperature of the coolant however the temperature gradient between heat source and condenser confirms that there is heat loss along the path from the heat source to the heat exchanger. Further increasing the liquid flow rate would not improve the internal forced convection heat transfer and attention should then be focused on enhancing the external forced convection (air-flow) over the condenser.

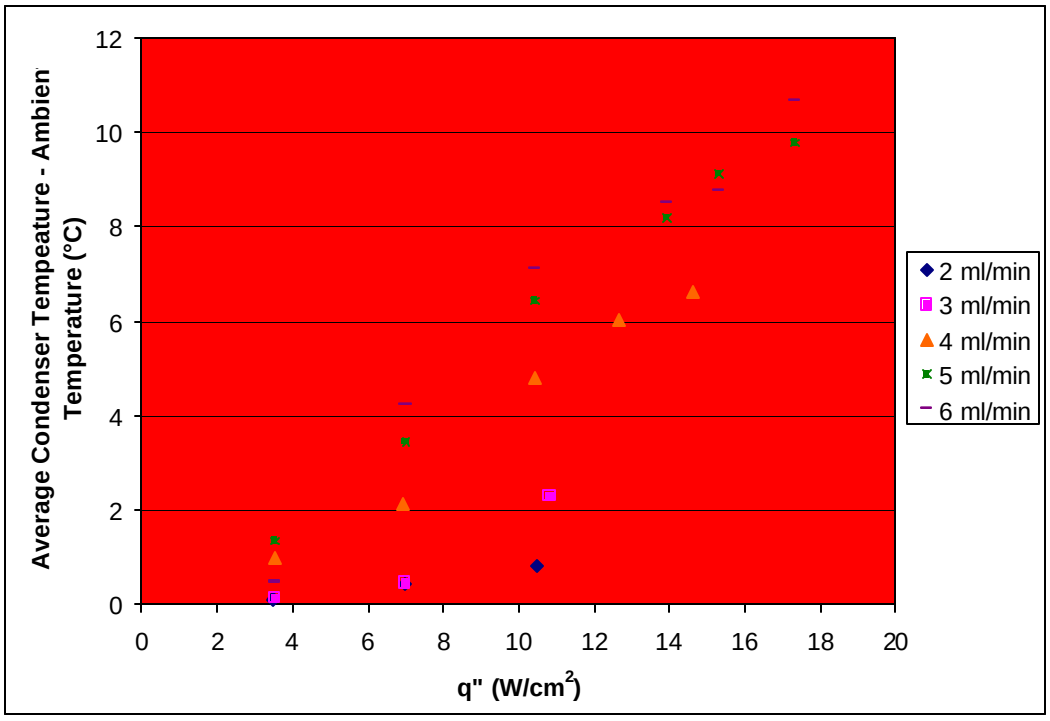

Figure 33 The effect of pump flow rate on average condenser temperature

4.3 Experimental Comparison of Two Condenser Designs

The inadequate demand for compact condensers, such as the one designed and tested in this project, results in very few commercially available compact heat exchangers and more costly customized fabrication jobs. A simple straight fin tube was procured from Fin Tube Products Inc. and its performance was compared to the customized serpentine fin tube condenser. The straight condenser is a helical-wound edge tension copper finned tube with a 9.53 mm outer diameter and 6.35 mm high fins (Figure 34). Although its surface area is 30% that of the serpentine condenser, the straight condenser offers less flow resistance which can reduce the pump power required for internal forced convection in the two-phase system.

Figure 34 Helical-wound straight copper condenser

The optimum parametric values for volume fill ratio and initial system pressure from prior experiments were applied to the straight condenser, while the flow rate varied from 3-5 ml/min. Figure 35 indicates lower thermal resistance values for the straight condenser at low heat fluxes, but then the system quickly approaches its limit (2.5 ?C/W) at approximately 10 W/cm^2 and begins to increase. At the highest heat flux value, 14

W/cm^2, and constant boundary conditions, the thermal resistance values for the serpentine condenser and the straight condensers are 2.8 ?C/W and 3.1 ?C/W respectively

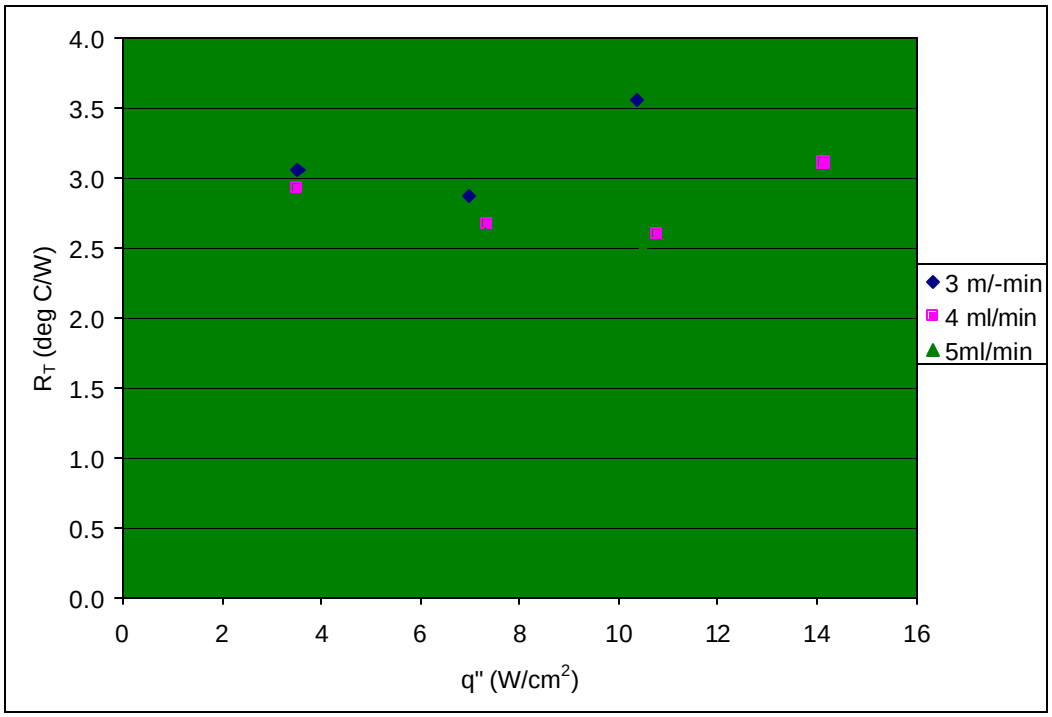

Figure 35 Performance of straight fin tube condenser

4.4 Two-Phase Cooling System with Micropump in Laptop

A micro diaphragm pump (Appendix B) and its small electronic control unit replaced the oversized Masterflex pump, and the entire cooling system is placed within the confines of the laptop cabinet with ventilation walls. The enclosed system was tested with the optimum parametric values to determine the system's performance with the micropump and also the effects of confinement on the forced convection air-cooling. There is an initial decrease in thermal resistance but the micropump system performs only marginally better than the gravity driven loop and can accommodate a mere 5.5 W/cm^2.

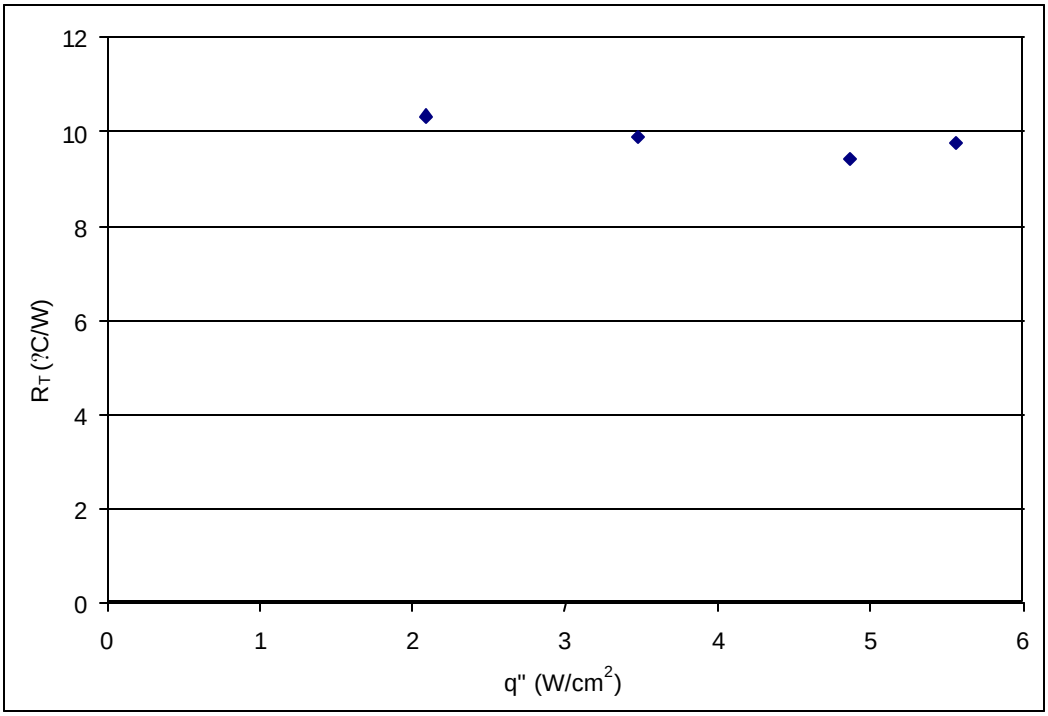

Figure 36 Two-phase closed system with micropump

4.5 Summary

A study of the effects of volume fill ratio, initial system pressure, and pump flow rate confirmed the importance of choosing design parameters that will optimize any system's performance. The two-phase closed loop performed optimally with a 50% fill ratio, low initial system pressure (? 30 kPa), and a pump flow rate of 0.1 cm^3/s (6 ml/min) to dissipate 25 W from the thermal test chip. Comparing a customized serpentine condenser to a more commercially available straight fin tube condenser did an analysis of surface area and internal flow resistance, which are both important factors in a two-phase system. The resistance value between the two condensers differed by only 2.5 ?C/W, but the larger surface area system peaked at a maximum heat flux of 17 W/cm^2 compared to 10 W/cm^2 for the straight fin tube.

CONCLUSION

In the design of a compact two-phase cooling system, initial numerical analysis showed the possibility of dissipating 30 W of heat from a specified volume of 200 cm^2, and computational software helped to evaluate and choose between two designs. Prototype tests showed the difficulty of ensuring a leak proof liquid cooling system for electronic devices, as well as the difference in ideal and actual performance for a complex cooling solution. The two-phase closed loop performed at its maximum when it was 50% filled with working fluid at 30 kPa initial system pressure with a pump at 0.1 cm^3/s (6 ml/min) flow rate to assist the liquid return to the evaporator. The pump is a critical component where physical size, reliability and cost are significant issues; it should also be leak free, small, and durable to meet system demands. Recent developments in technology have produced diaphragm, peristaltic, and electrokinetic micro pumps but reliability and performance improvements are necessary to ensure an efficient cooling system.

Numerical analysis of airflow across the condenser provided valuable information for fan orientation and flow rate, as well as location of vents along the walls of the laptop enclosure. A simple modification in the location of the vents produced approximately 20% increase in total heat transfer. The actual flow patterns through the fins showed the large pressure drop across the condenser that could be addressed in the actual design of the condenser or as a peripheral to the cooling solution. The two-phase closed loop system can dissipate 25 W of heat from a thermal chip which can be enhanced by

extending the cooling system and dissipating more heat with a cold plate or phase change material (PCM) from the display panel.

APPENDICES

APPENDIX A

TECHNICAL DOCUMENTAION ON MICRO DIAGHRAGM PUMP AND PUMP CONTROL

XXS2000 micro diaphragm pump

Main Features:

- ?? self-priming
- ?? tolerant of gas bubbles
- ?? low power consumption / piezo actuated
- ?? small dimensions
- ?? pumps gasses and liquids alike
- ?? high chemical resistance

Technical Specifications:

max flow rate [microLiters/min]:	6,000 (water at 20 degree C)
max back pressure [hPa]:	350 (water at 20 degree C)
max. particle size [micrometers]:	10
max. viscosity [mPas]:	~350
lifetime [strokes]:	> 10E8
operating temperature [degree C]:	10 – 50
media temperature [degree C]:	10 – 50
material:	
wetted parts:	COC (Topas)
protective cover:	COC
weight (without cable) [g]:	3

Connections:

fluidics	
outer diameter [mm]:	2.0
inner diameter [mm]:	0.8
length [mm]:	4.4
SMB-connector (female)	SMB-type, RF coaxial, crimp, plug (female), Telegartner J01161A0021

XXS-EF20F Specifications
Electronic Pump Control

Main Features:

- ?? variable frequency adjustment
- ?? compact size
- ?? low power consumption

Technical Specifications:

supply voltage [V]:	4.5-7 controlled DC or 6 V battery voltage
quiescent current consumption [mA]:	< 200
current consumption [mA]:	50 (at 0.5 Hz, 6 V)
output voltage [V]:	+340 +/- 2% (controlled) -70 to -90 (depending on supply voltage)
frequency range [Hz]:	0 to 200
input resistance for control input [kOhm]:	30
input resistance shutdown [kOhm]:	50
operating temperature [degree C]:	+5 to +40
storage temperature [degree C]:	-25 to +85
weight [g]:	25

APPENDIX B

LAPTOP SYSTEM LAYOUT

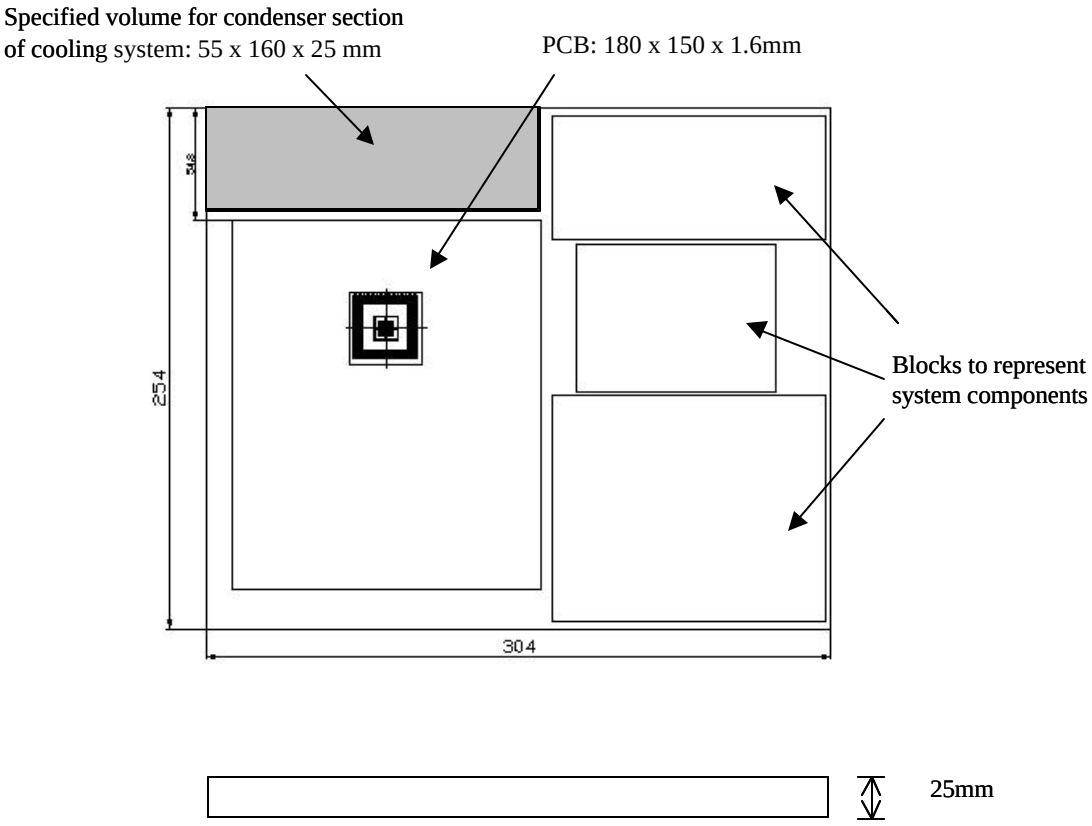

APPENDIX C

FAN CURVE DATA

Table 3 Specifications for 25 x 25 x 10 mm fan

Green Motor Series (MagLev)

Model	P/N	Bearing ● VAPO ○ BALL ◔ 2BALL	Rating Voltage (VDC)	Power Current (AMP)	Power Consumption (WATTS)	Speed (RPM)	Air Flow (CFM)	Static Pressure (Inch-H_2O)	Noise (dBA)	Weight (g)
GM0502PFV1-8		●	5	0.13	0.7	13000	3.5	0.25	23.0	7.2
GM0502PFV2-8		●	5	0.08	0.4	10000	3.0	0.18	16.0	7.2
GM0502PFV3-8		●	5	0.04	0.2	7000	2.3	0.11	9.5	7.2
GM0502PFB1-8		○	5	0.13	0.7	13000	3.5	0.25	25.0	7.2
GM0502PFB2-8		○	5	0.08	0.4	10000	3.0	0.18	18.0	7.2
GM0502PFB3-8		○	5	0.04	0.2	7000	2.3	0.11	11.0	7.2

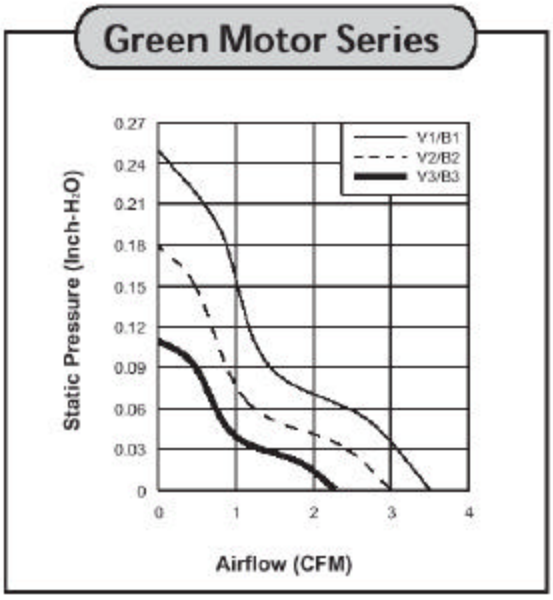

Figure 37 Performance curve for 25 x 25 x 10 mm fan

APPENDIX D

CHARACTERISTICS OF REFRIGERANTS AND MAXIMUM CONTAMINANT LEVELS

Table 4 Characteristics of Refrigerants [24]

	Reporting units	Reference (subclause)	R11	R12	R13	R22	R113	R114
Characteristics*:								
Boiling Point*	F @ 1.00 atm		74.9	-21.6	-114.6	-41.4	117.6	38.8
	deg.C @ 1.00 atm		23.8	-29.8	-81.4	-40.8	47.6	3.8
Boiling Point Range*	K		0.3	0.3	0.5	0.3	0.3	0.3
Typical Isomer Content	By weight						0-1%	0-30%
							R113a	R114a
Vapor phase contaminants:								
Air and other non-condensables	% by volume @ 25 deg.C	5.9	N/A**	1.5	1.5	1.5	N/A**	1.5
Liquid phase contaminants:								
Water	ppm by weight	5.4	20	10	10	10	20	10
All other impurities including refrigerants.	% by weight	5.10	0.50	0.50	0.50	0.50	0.50	0.50
High boiling residue	% by volume	5.7	0.01	0.01	0.05	0.01	0.03	0.01
Particulates/solids	Visually clean to pass	5.8	Pass	Pass	Pass	Pass	Pass	Pass
Acidity	ppm by weight	5.6	1.0	1.0	1.0	1.0	1.0	1.0
Chlorides***	No visible turbidity	5.5	Pass	Pass	Pass	Pass	Pass	Pass

*Boiling points and boiling point ranges, although not required, are provided for informational purposes.
**Since R11, R113 and R123 have normal boiling points at or above room temperature, non-condensable determinations are not required for refrigerants.
***Recognized Chloride level for pass/fail is 3ppm.

APPENDIX E

SATURATED PROPERTIES OF FC72

T (K)	P (Atm)	ρ_l (kg/m^3) [1]	ρ_g (kg/m^3) [1]	C_l [J/(kg·K)] [2]	h_{fg} (J/kg) [1]	σ (N/m) [3] x 10^3	ν_l (m^2/s) [4] x 10^6	k [W/(m·K)] [5] x 10^2
273.15	0.0851	1755.2917	1.3708	1011.0	99214.8	13.342	0.5410	6.0167
283.15	0.1438	1719.7774	2.2336	1026.5	96850.5	12.412	0.4652	5.9050
293.15	0.2323	1691.5423	3.4844	1041.9	94400.0	11.496	0.4060	5.7933
303.15	0.3606	1669.1213	5.2305	1057.3	91851.0	10.595	0.3601	5.6816
313.15	0.5404	1649.6846	7.5886	1072.8	89203.5	9.708	0.3245	5.5699
323.15	0.7850	1631.4779	10.6830	1088.2	86432.8	8.838	0.2961	5.4582
333.15	1.1091	1613.6687	14.7935	1103.7	83563.6	7.985	0.2719	5.3466
343.15	1.5288	1593.2521	20.2385	1119.1	80583.6	7.150	0.2499	5.2349
353.15	2.0615	1568.9894	27.2035	1134.5	77517.4	6.334	0.2306	5.1232
363.15	2.7255	1539.1580	35.9758	1150.0	74389.6	5.538	0.2111	5.0115
373.15	3.5410	1501.1038	46.9957	1165.4	71224.9	4.766	0.2092	4.8999
383.15	4.5290	1452.9915	60.6255	1180.9	67715.3	4.018	0.2084	4.7882
393.15	5.7127	1394.0139	77.4964	1196.3	64316.6	3.297	0.2079	4.6765
403.15	7.1173	1320.9013	98.5507	1211.8	60154.5	2.606	0.2076	4.5648
413.15	8.7709	1232.7774	125.5864	1227.2	55167.3	1.952	0.2074	4.4531
423.15	10.7059	1127.6949	162.0437	1246.6	48985.6	1.339	0.2072	4.3415
433.15	12.9609	1003.2458	215.2171	1258.1	41141.5	0.779	0.2070	4.2298
443.15	15.5839	857.7195	303.1384	1273.5	30268.1	0.294	0.2069	4.1181
451.65	18.1659	613.4969	612.5023	1286.7	0	0	0.2068	4.0232

1. Converted from "Table 13A: Saturated Properties of FC-72", 3M Product Manual, "FLUORINERT® Electronic Liquids", pp. 57, 1987.

2. C_l = 589.18 + 1.5443 T(K), correlated from Fig. 4, 3M Product Manual, "FLUORINERT® Electronic Liquids", pp. 14, 1987.

REFERENCES

1. Shoji, H. *The Future of The Notebook Computer*. in *IEEE International Solid-State Circuits Conference*. 1991.
2. Corporation, I., *http://www.intel.com/products/mobiletechnology/form.htm?iid=ipp_mobiletech+use_more&*, in *Mobile Technology*.
3. Corporation, I., *Mobile Pentium III Processor in BGA2 and MicroPGA2 Packages*. 2000.
4. Chan, L., *Intel Celeron M Processor Debuts.* 2004.
5. Danielson, R.D., Tousignant, L., and Bar-Cohen, A. *Saturated Pool Boiling Characteristics of Commercially Available Perfluorinated Liquids*. in *Proceedings of ASME/JSME Thermal Engineering Joint Conference*. 1987.
6. Simons, R.E., *Direct Liquid Immersion Cooling for High Power Density Microelectronics*. 1996.
7. Ali, A., DeHoff, A., Grubb, K., *Advanced Heat Pipe Thermal Solutions for Higher Power Notebook Computers*. 1999.
8. Xie, H., Aghenndeh, M., Lui, W., and Haley, K., *Thermal Solutions to Pentium Processor in TCP in Notebooks and Sub-Notebooks*. IEEE Transactions on Components and Packaging and Manufacturing Technology, 1996. **Part A, Vol. 19,**(Number 1): p. 201-210.

9. Mochizuki, M., Saito, Y., Goto, K., Nguyen, T., Ho, P., Malcolm, M., Morando, M.P., *Hinged Heat Pipes for Cooling Notebook PCs*. IEEE 13th SEMI-THERM Symposium, 1997: p. 64-72.

10. Staudter, T., http://www.research.ibm.com/thinkresearch/pages/2001/20010808_cooling.shtml, IBM Think Research.

11. Nguyen, T., Mochizuki, M., Mashiko, K., Saito, Y. *Use of Heat Pipe/Heat sink for Thermal Management of High Performance CPUs.* in *IEEE 16th SEMI-THERM Symposium*. 2000.

12. *Intel Mobile Cooling Technology Provides Higher Performance in Thinner and Cooler Notebooks,* in *Intel Mobile Cooling Technology Initiatives*.

13. Nguyen, T., Mochizuki, M., Mashiko, K., Saito, Yuji., Sauciuc, I., Boggs, R., *Advanced Cooling System Using Miniature Heat Pipes in Mobile PC*. IEEE Transactions on Components and Packaging Technology, 2000. **23**(1).

14. Kuzmin, G. *Oasis™ cooling packaging technology for notebook computers*. in *Proceedings of the Electro'94 International Conference*. 1994. Boston, MA, USA: IEEE, Piscataway, NJ, USA.

15. Jiang, L., Mikkelsen, J., Koo, J.M., Huber, D., Yao, S., Zhang, L., Zhou, P., Maveety, J.G., Prasher, R., Santiago, J.G., Kenny, T.W., and Goodson, K.E., *Closed-Loop Electroosmotic Microchannel Cooling System for VLSI Circuits*. IEEE Transactions on Components and PackagingTechnologies, 2002. **25**(3): p. 347-355.

16. Kondo, Y. *Innovation Technology in Electronic Equipment*. in *4th ASME/JSME Joint Fluids Engineering Conference*. 2003. Honolulu, Hawaii: New York : American Society of Mechanical Engineers, c2003.

17. Nakayama, W., Nakajima, T., and Hiraasawa, S., *Heat Sink Studs Having Enhanced Boiling Surfaces for Cooling Microelectronic Components.* ASME Paper, 1984. **No. 84-WA/HT-89**.

18. Pal, A., Joshi, Y., Beitelmal, M.H., Patel, C.D., Wenger, T. *Design and Performance evaluation of a compact thermosyphon*. in *IEEE Transactions on Components and Packaging Technologies*. 2002.

19. Gunther, S.H., Binns, F., Carmean, D.M. and Hall, J.C., *Managing the Impact of Increasing Microprocessor Power Consumption.* 2001.

20. Arik, M., Bar-Cohen, A. *Immersion Cooling of High Heat Flux Microelectronics with Dielectric Liquids*. in *International Symposium on Advanced Packaging Materials*. 1998.

21. Saylor, J.R., Bar-Cohen, A., Lee, T-Y., Simon, T.W., Tong, W., and Wu, P-S. *Fluid Selection and Property Effects in Single and Two-Phase Immersion Cooling*. in *IEEE Transactions on Components, Hybrids, and Manufacturing Technology*. 1988.

22. *Air Cooling Technology for Electronic Equipment*, ed. S.J. Kim, Sang, W.L. 1996: CRC Press. 8-11.

23. *Characteristics of Refrigerants and Maximum Contaminant Levels*.

24. *Specifications for Fluorocarbon Refrigerants.* 1994, Compliance Resource Center.